

# Inferring the tree regeneration niche from inventory data using a dynamic forest model

Yannek Käber<sup>1,2</sup>, Florian Hartig<sup>3</sup>, Harald Bugmann<sup>1</sup>

<sup>1</sup>Forest Ecology, Institute of Terrestrial Ecosystems, Department of Environmental Systems Science, ETH Zurich, Zurich, 8092, Switzerland

<sup>2</sup>Chair of Silviculture, Faculty of Environment and Natural Resources, University of Freiburg, Freiburg, 79106, Germany

<sup>3</sup>Theoretical Ecology Lab, Faculty of Biology and Pre-Clinical Medicine, University of Regensburg, Regensburg, 93053, Germany

10 *Correspondence to:* Yannek Käber (y.kaeber@posteo.de)

**Abstract.** The regeneration niche of trees is governed by many processes and factors that are challenging to determine. Besides a species's geographic distribution, which determines if seeds are available, a myriad of local processes in forest ecosystems (e.g., competition, pathogens) exert influence on tree regeneration. Consequently, the representation of tree regeneration in dynamic forest models is a notoriously complicated process which often involves many subprocesses that are often data deficient. The ForClim forest gap model solved this problem by linking species traits to regeneration properties. However, this regeneration module was never validated with large-scale data. Here, we compare this trait-based approach with an inverse calibration approach, where we estimate regeneration parameters directly from a large dataset of unmanaged European forests. The inverse calibration was done using Bayesian inference, estimating shade and drought tolerance as well as the temperature requirements for 11 common tree species along with the intensity of regeneration (i.e., the maximum regeneration rate). We find that the parameters determining species' light niche (i.e., light requirements) are similar between the trait based and calibrated values for both model variants, but only a more complex model variant that included competition between recruits led to plausible estimates of the drought niche. The trait-derived temperature niche did not match to the estimates from either model variant using inverse calibration. The parameter estimates differed between the complex and the simple model, with the estimates for the complex model being closer to the trait-based parameters. In both model variants, the calibration strongly changed the parameters that determine regeneration intensity compared to the default.

We conclude that the regeneration niche of trees can be recovered from large forestry data in terms of the stand-level parameters light availability and regeneration intensity, while abiotic drivers (temperature and drought) are more elusive. The higher performance (better fit to hold-out) of the inversely calibrated models underpins the importance of informing dynamic models by real-world observations. Future research should focus on an even larger environmental coverage of observations of demographic processes in unmanaged forests to verify our findings at species range limits under extreme climatic conditions.

## Introduction

Predictions of species range shifts and forest dynamics under climate change require process-based models that account for the complex feedback between stand dynamics, soils, and climate (Morin and Thuiller, 2009). In this context, tree regeneration is particularly important because of its key role in species range shifts (McDowell et al., 2020), and forest resilience to climate change (i.e., reorganisation after disturbances; Seidl and Turner, 2022). Yet, tree regeneration is an uncertain and convoluted process (Price et al., 2001; König et al., 2022), as shown by numerous studies that yield different results depending on the site, species, and spatial and temporal scale that is considered (Clark et al., 1999; Lett and Dorrepaal, 2018). The reason for these divergences among observations and experimentation is a) that many seemingly stochastic regeneration processes are actually controlled by biotic and abiotic conditions that vary across a wide range of temporal and spatial scales (Grubb, 1977; Hart et al., 2017), coupled with b) the lack of suitable data to consistently study these processes on different scales (Clark et al., 1999). A challenge that hinders progress on these questions is that a tree's regeneration niche is generally driven by many factors and lacks a clear definition that distinguishes it from a plant's full niche (Grubb, 1977). Instead, differences between Grubb's niche types are continuous (see also ontogenetic shifts in environmental preferences, Heiland et al., 2022) and valid only conceptually. At the same time, Grubb's definition of the regeneration niche as "an expression of the requirements for a high chance of success in the replacement of one mature individual by a new mature individual of the next generation [...]" provides a coherent framework to which regeneration models can be related.

Regeneration in most Dynamic Forest Models (DFMs) is captured in a relatively simple manner (compared to growth and mortality of adult trees) and, due to the lack of detailed process data, mostly phenomenologically (König et al., 2022). Nevertheless, even these simplified representations of tree regeneration are characterized by widely different levels of complexity (Bugmann and Seidl, 2022). Typically, the representations of regeneration in DFMs are based on knowledge that is abstracted to an aggregate over many processes (Price et al., 2001). DFMs usually simulate regeneration via binary, count, or hurdle models. Such probabilistic models simulate the occurrence of small trees at certain size thresholds as a function of environmental variables and sometimes dispersal, vegetative reproduction, or browsing. The complexity of these models is characterized by the different definitions of the relation between environmental variables and species' regeneration probability. Consequently, there is a wide range from very simple models that use binary threshold values for one or very few variables (e.g., FORMIND, Köhler and Huth, 1998), to highly complex models with continuous transitions from unsuitable to suitable regeneration conditions comprising many variables (e.g., iLAND, Seidl et al., 2012). In addition, the actual regeneration amount is often calculated invoking random numbers, which leads to high stochasticity and renders the validation of tree regeneration patterns in DFMs challenging. Bugmann and Seidl (2022) and Hanbury-Brown et al. (2022) provide a comprehensive overview of regeneration models.

In this study, we focus on the relation between tree species' regeneration success and environmental variables in DFMs. For this purpose, we aim to disentangle the effects of large- and small-scale environmental drivers on tree regeneration based on regeneration data that stem from natural conditions, i.e. unmanaged forests. In conjunction with such data, DFMs can be used

65 to assess how simulated natural regeneration relates to real-world observations. First, DFMs represent complex stand-  
environment feedbacks explicitly, which puts the quantified effects in the context of specific processes. For example, species'  
shade tolerance estimates will only be constrained by the actual available light and not by any other confounding factors. Thus,  
it opens up opportunities for more nuanced inference on processes, instead of yielding loose associations between observed  
70 regeneration patterns and environmental drivers. Second, using data from unmanaged forests minimizes the confounding  
influence of management on demographic processes. Specifically, the promotion of certain species or individual trees through  
planting or thinning are absent in unmanaged forests.

Over the past decade, robust methods for evaluating stochastic models of ecological processes with data have been developed  
(cf. Hartig et al., 2011). Yet, only a few studies have confronted tree regeneration models with forest inventory data (Rüger et  
al., 2009; Díaz-Yáñez et al., in press). An important reason is the issue of elucidating the drivers of ecological processes at  
75 different spatial and temporal scales mechanistically, as the apparent stochasticity makes it challenging to retrieve signal from  
the data (Hart et al., 2017; Oberpriller et al., 2021; Shoemaker et al., 2020). Specifically, trade-offs between meaningful  
observations for key small-scale processes such as light competition, browsing, microclimate (e.g., frost events) and the  
coverage of macroclimatic gradients at which dispersal and plant migration take place impede a comprehensive analysis across  
the stages of tree regeneration (Clark et al., 1999). Consequently, there is a need to advance the frontier of evaluating tree  
80 regeneration in DFMs with data (cf. Díaz-Yáñez et al., in press).

In the DFM ForClim (Huber et al., 2020), which we use as a case study, the regeneration niche is captured, among other  
factors, based on light availability, water availability, and summer temperature conditions. It is derived from trait values for  
shade tolerance, drought tolerance, and minimum degree-days (e.g., Leuschner and Ellenberg, 2017). The model is highly  
sensitive to the values of these parameters (cf. Huber et al., 2018), which adds weight to their detailed evaluation based on  
85 real-world observations. For traits directly linked to a specific, explicitly modelled process, such as the relationship between  
species' shade tolerance and light availability, a higher predictive power is anticipated. In contrast, traits influencing multiple  
processes tend to exhibit lower predictive power. An example of this is the intricate relationships involving species' temperature  
requirements, frost tolerance, and drought tolerance, all of which interact with factors such as precipitation and temperature  
(cf. Yang et al., 2018). Functional traits have successfully been applied in simple dynamic models of annual plant communities  
90 (e.g., Chalmandrier et al., 2021), thus underpinning the validity of trait-based approaches for modelling plant demography.

In ForClim, the interplay between the traits of multiple species is implemented in two variants, i.e. a simple and a complex  
approach for capturing regeneration processes. In the simple approach, the relation between traits and environmental conditions  
is defined using *binary thresholds* and competition among regenerating trees *is not* considered. In the complex approach, the  
relation between traits and environmental conditions is defined with *continuous* transitions between suitable and unsuitable  
95 regeneration conditions, and competition among regenerating trees *is* considered (Huber et al., 2020). Interestingly, in both  
variants the link between traits and processes leads to ecologically plausible emergent properties of simulated Potential Natural  
Vegetation along elevational gradients in the Swiss Alps (Huber et al., 2020) and elsewhere (Bugmann and Solomon, 2000).  
While empirical studies based on plot-level data have provided valuable insights into large-scale regeneration patterns (Zell et

al., 2019; Käber et al., 2021), it remains unclear whether DFMs can match such empirical data. A comparison of many DFMs  
100 with data of unmanaged European forests shows that mismatches exist, yet the reasons for these mismatches remain vague  
(Díaz-Yáñez et al., in press).

Here, we evaluate possible reasons for mismatches between process formulations and observations by comparing two  
approaches for parameterizing the regeneration niche in ForClim: (1) a trait-based approach, where the regeneration niche is  
based on trait values determined *a priori* from ecological knowledge, and (2) an inverse calibration approach, where the trait  
105 values are derived *a posteriori* using a novel observational data set of demographic processes in European unmanaged forests  
that covers unprecedented spatial and temporal scales (Käber et al., 2023). Specifically, we address two research questions.

- How does the regeneration niche that is emerging from the inverse calibration differ compared to the niche defined  
by species' traits?
- Does a more complex regeneration model that includes competition feature a higher performance compared to a  
110 simple regeneration model without competition?

## Methods

### Data

#### Forest inventory data

We used records of tree recruitment from 6,540 forest inventory plots covering 299 strict forest reserves that are curated by 18  
115 European research institutions in the context of the European Forest Research Initiative (EuFoRIa, [www.euforia-project.org](http://www.euforia-project.org))  
(Käber et al., 2023). Depending on the forest inventory design, different diameter thresholds (DBH, diameter at breast height)  
were used as the calliper limit in the inventories (i.e., 4, 7 or 10 cm). These inventory plots were aggregated or split into  
units of ca. 1 ha to obtain samples of similar spatial extent (Käber et al., 2023) that reduce the stochasticity in the data and thus  
increase the stability of the signal used for model evaluation. After data processing (Käber et al., 2023), 865 plots were  
120 available for this study. Some trees within these plots had implausible DBH measurements (e.g., annual DBH growth was  
unrealistically high ( $\Delta\text{DBH} > 2$  cm/year) or negative ( $\Delta\text{DBH} < -0.1$  cm/year), which required the exclusion of some plots. This  
allowed us to obtain a data set where all observations are in an ecologically plausible range.

We defined two criteria for selecting plots suitable for the study. The first criterion evaluated the number of trees with  
implausible measurements relative to the total number of measured trees and observed basal area: at least 95 % of all trees  
125 needed to have plausible measurements together with at least 95 % of the basal area being comprised of trees with plausible  
DBH measurements. The second criterion evaluated the number of trees with implausible measurements relative to the plot  
area: the maximum number of trees with implausible measurements per ha allowed in the data set was defined as the 75<sup>th</sup>  
percentile of trees with implausible measurements per ha (which amounted to 14.31 ha<sup>-1</sup>). The second criterion was defined

because some plots did not fulfil the first criterion although they had a relatively low number of trees with implausible measurements per ha. These were particularly large plots with low tree number per ha ( $N = 51$ ). After plot selection, all trees with implausible DBH measurements of the selected plots were removed.

The final number of sites considered was 696 with sufficient information on tree regeneration for 11 tree species. All other species were aggregated in an extra category (“other” species). About half of the sites (353) were used for calibration (training data), and the other half (343) for evaluation (test data). We split the sites so that the variation of the represented inventory data sets (i.e., the individual data associated to one research institution) and DBH thresholds was similar in both test and training data. This also resulted in similar variations of environmental conditions because each inventory data set (from a given institution) represents a specific region with similar environmental conditions.

### **Environmental input data**

ForClim contains a stochastic weather generator where the long-term averages and standard deviations of monthly mean temperature and log-transformed precipitation sums along with their cross-correlation serve as input (Bugmann, 1994; Risch et al., 2005). These climatic input variables were derived from the CHELSA data set version 2 (Karger et al. 2017) with a horizontal resolution of 30 arc seconds. The plot’s slope and aspect (represented as  $kSlAsp$  in the model; cf. Bugmann, 1994) are input variables as well; they were derived from the Copernicus digital elevation model EU-DEM (EU-DEM 2020) with a spatial resolution of 25 m, which was further processed with QGIS (QGIS Development Team 2022) to calculate slope and aspect on a spatial resolution of 100 m. The so-called “bucket size”, i.e., the plant-available water storage capacity of the soil, was derived with a Random Forest model trained with expert assessments of the soil quality of a subset of the plots (cf. Käber et al., 2023a).

### **The forest gap model ForClim**

ForClim is a dynamic vegetation model that simulates the processes of growth, mortality, and regeneration (often also called “establishment”) of individual trees via species-specific size cohorts (Bugmann, 1994). ForClim classifies as a forest gap model (Shugart, 1984) and simulates forests on independent patches, each of a size of 800 m<sup>2</sup>. By default, 100 patches (i.e., 8 ha) comprise a forest stand to obtain realistic averages of forest dynamics across patches. The model uses an annual time step and represents trees as cohorts with the properties number of trees (Trs), their diameter at breast height (DBH), height, leaf area, and stress level. Here, we used two variants of the regeneration module within ForClim v4.0.1 (Huber et al., 2020).

### **The two regeneration models**

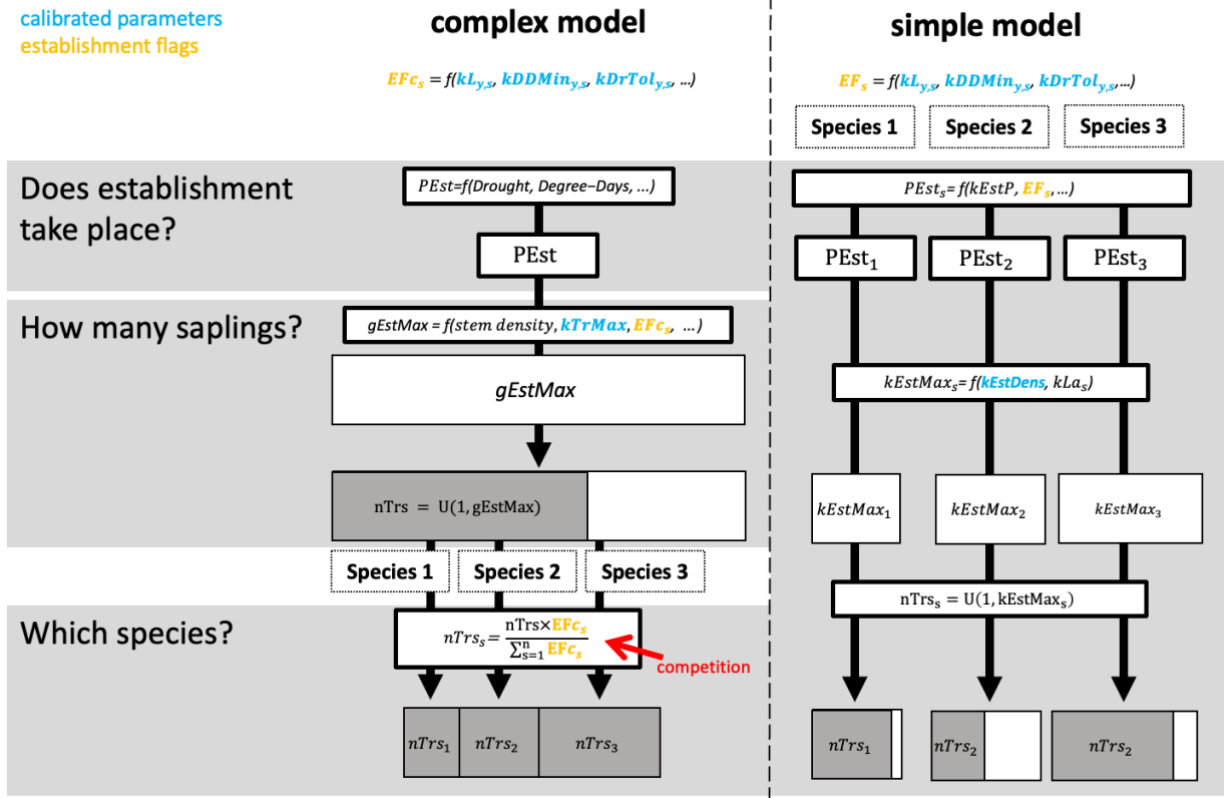
The ForClim regeneration module initiates new cohorts of trees based on a) site variables for climate and soil in combination with b) species traits, and c) state variables of forest structure. The species traits of drought tolerance, temperature, and light requirements originate from indicator values of Ellenberg (1986) (cf. latest translated edition, Leuschner and Ellenberg, 2017) and the FORECE model (Kienast, 1987). They define thresholds (so-called “establishment flags”, EFs) that must be fulfilled

160 for a species to qualify for establishment at a DBH of 1.27 cm. For example, if a species has an EF of 10 % available light to regenerate the EF will be fulfilled if the available light is  $\geq 10\%$ , if the available light is  $< 10\%$  the species EF is not fulfilled (cf. the detailed description of establishment flags below). In this study, we focus on a simple and a more complex variant of the regeneration model. Below, a brief summary of the two models is provided, followed by an explanation of the EFs investigated here. For more details, see Figure 1, Appendix B, and the original documentation of the simple and complex  
165 model in Bugmann (1994) and Huber et al. (2020), respectively.

The simple model simulates tree regeneration for each species independently and corresponds to the original ForClim *establishment module* in Bugmann (1994), which is the same as model variant 1 in Huber et al. (2020). EFs in this model indicate either “suitable” or “not suitable”, i.e., they are binary. In a first step, the annual regeneration probability (kEstP), modulated by species-specific EFs, determines whether regeneration for each species takes place. Second, if regeneration of a  
170 species takes place, the potential maximum number of new trees for that species is calculated from (1) a regeneration intensity parameter (kEstDens, which is the maximum tree establishment density per species [ $m^{-2}yr^{-1}$ ]) and (2) the species-specific successional strategy (i.e., shade-intolerant species have a higher number of seeds and thus offspring compared to shade-intolerant species). Third, the actual number of new trees *per species* is derived by drawing a random number between 1 and the potential maximum number of trees for each species.

175 The complex model includes a mechanism for competition and was first introduced as variant 11 in Huber et al. (2020). EFs in this model are continuous, which allows for a more nuanced gradient from “suitable” to “not suitable”. In the first step, kEstP as modulated by a drought index and degree-days is used to determine if regeneration for any species takes place. Second, if regeneration does take place, the total potential number of new trees over all species is calculated from (1) a regeneration intensity parameter (kTrMax, which is the absolute maximum number of trees [ $ha^{-1}$ ]) and (2) a drought index,  
180 degree-days, and the continuous EFs. The actual number of new trees *over all species* is then derived by drawing a random number between 1 and the potential maximum number of trees over all species. Third, the number of new trees per species is calculated by multiplying the actual number of trees over all species by the species-specific ratio of each species’ EF and the sum over the EFs of all species.

calibrated parameters  
establishment flags



185 **Figure 1: Simplified visual representation of the simple and complex regeneration model variants of ForClim. As full description of the models is provided below.**

### Establishment flags regarding light, temperature, and soil moisture

In the present study, we focus on three of the five EFs that are used in the two models (Table 1). The definition of these three EFs (for light, drought, and degree-days) is given below.

190 The available light establishment flag (ALEF) evaluates whether the sunlight available at the forest floor ( $gAL_0$ , see p. 63 in Bugmann (1994) for details) matches a parameter for species' light requirements to regenerate ( $kL_{y,s}$ ).  $kL_{y,s}$  is derived from indicator values regarding the light requirements of young trees ( $L_s$ ) ranging from 1 to 9 (Leuschner and Ellenberg, 2017) with

$$kL_{y,s} = \begin{cases} 0.025 \cdot (L_s - 1) & L_s < 5 \\ 0.1 \cdot L_s - 0.4 & \text{else} \end{cases} \quad \text{eq. 1)}$$

For each species  $s$ , the binary EF ( $ALEF_{b,s}$ ) in the simple model is calculated with

$$ALEF_{b,s} = \begin{cases} 0 & gAL_0 < kL_{y,s} \\ 1 & \text{else} \end{cases} \quad \text{eq. 2)}$$

while the continuous EF ( $ALEF_{c,s}$ ) in the complex model is calculated with

$$ALEF_{c,s} = \begin{cases} 0 & gAL_0 < kLy,s \\ 1 & gAL_0 \geq kLy,s + 0.5, \\ \frac{gAL_0 - kLy,s}{0.5} & kLy \leq gAL_0 < kLy,s + 0.5 \end{cases}, \quad \text{eq. 3}$$

195 where the value 0.5 refers to the highest  $kLy,s$  (cf. eq. 1) and serves as a buffer for the transition from zero to one.

The degree-days establishment flag (DDEF) evaluates whether the annual degree-day sum (gDD, see p. 81 in Bugmann (1994) for details) matches the species' minimum degree-day requirement (kDDMin). The values of kDDMin originate from Kienast (1987), who derived climatic variables from Müller (1982) and Rudloff (1981) for multiple geographic locations and elevations within the species' distribution range (Ellenberg and Klötzli, 1972; Meusel et al., 1965). This approach was further improved  
200 by applying a site-specific bias correction (Bugmann, 1994). Note that this parameter has never been modified to reflect possible deviations regarding the regeneration niche. In this study, we distinguish between the original parameter (kDDMin of adults) and kDDMin<sub>y</sub>, which applies to the regeneration. For each species *s*, the binary EF (DDEF<sub>b,s</sub>) in the simple model is calculated with

$$DDEF_{b,s} = \begin{cases} 0 & kDDMin_{y,s} \geq gDD \\ 1 & \text{else} \end{cases}, \quad \text{eq. 4}$$

while the continuous EF (DDEF<sub>c,s</sub>) in the complex model is calculated with

$$DDEF_{c,s} = \begin{cases} 0 & kDDMin_{y,s} \geq gDD \\ 1 & gDD \geq kDDMin_{y,s} + 256, \\ \frac{gDD - kDDMin_{y,s}}{256} & kDDMin_{y,s} < gDD < kDDMin_{y,s} + 256 \end{cases}, \quad \text{eq. 5}$$

205 where the value 256 refers to the lowest  $kDDMin_{y,s}$  and serves as a buffer for the transition from zero to one.

Lastly, the soil moisture establishment flag (SMEF) evaluates whether the drought index (gDr), defined as the ratio of actual evapotranspiration and water demand by the atmosphere (i.e., potential evapotranspiration) matches the species' threshold for this index, i.e., the drought tolerance (kDrTol). The original trait values for drought tolerance range from 1 to 5 (Leuschner and Ellenberg, 2017) and were scaled between 0.06 and 0.3 (i.e., 30 %). The evolution of the formulation of the drought index  
210 is documented in Bugmann (1994); Bugmann and Cramer (1998); and Bugmann and Solomon (2000), including its integration in the regeneration model (Didion et al., 2009a). Similar to DDEF, the original parameter (kDrTol of adults) and kDrTol<sub>y</sub> are distinguished here, and the latter applies to regeneration only. For each species *s*, the binary EF (SMEF<sub>b,s</sub>) in the simple model is calculated with

$$SMEF_{b,s} = \begin{cases} 0 & gDr > kDrTol_{y,s} \\ 1 & \text{else} \end{cases}, \quad \text{eq. 6}$$

while SMEF<sub>c,s</sub> in the complex model is calculated with

$$\text{SMEF}_{c,s} = \begin{cases} 0 & gDr > kDrTol_{y,s} \\ 1 & gDr \leq kDrTol_{y,s} - 0.08 \\ \frac{kDrTol_{y,s} - gDr}{0.08} & kDrTol_{y,s} > gDr > kDrTol_{y,s} - 0.08 \end{cases}, \quad \text{eq. 7}$$

215 where the constant of 0.08 indicates the lowest  $kDrTol_{y,s}$  and serves as a buffer for the transition from zero to one, i.e., the EF being fulfilled or not (cf. Huber et al., 2020).

The two EFs in the model that are not considered here are the winter temperature establishment flag (WTEF), which depends on minimum tolerated winter temperature and chilling requirements (Bugmann, 1994; Bugmann and Cramer, 1998; Kienast, 1987); and the browsing pressure flag, which depends on the species' susceptibility to ungulate browsing (Didion et al., 2009b).  
 220 WTEF is correlated with DDEF and excluded from the calibration to avoid too many degrees of freedom. We therefore used the default parameterization for WTEF. Because no site information on browsing pressure was available, we decided against using this factor in the calibration. Instead, we kept browsing pressure constant across all sites at its default value of 20 %.

**Table 1: Description of ForClim model parameters that are considered for calibration.**

Model variant		Description	Default	Prior	Comment
	$kDrTol_y$	Species drought tolerance	0.08-0.37	0.001-0.02 (0.001-0.4)	The species' drought tolerance and a drought index determine the EF for drought (Bugmann, 1994; Huber et al., 2020).
simple & complex	$kDDMin_y$	Species minimum degree-days	385-1339	100-1500	The species' minimum degree-day sum and degree-days determine the EF for temperature (Bugmann, 1994; Huber et al., 2020).
	$kLy$	Species light requirements	0.03-0.4	0.001-0.5	Species' light requirements and available light on the forest floor determine the EF for light (Bugmann, 1994).
complex	$kTrMax$	Maximum Number of Trees per ha	30000	500 – 50000	Maximum number of trees per ha refers to the number of trees regardless of the species. It also includes the trees that are already present on the patch (Huber et al., 2020).
simple	$kEstDens$	Maximum Establishment Density [trees/(m <sup>2</sup> ·yr)]	0.006	0.001- 0.2	Maximum tree establishment density is defined per species (Bugmann, 1994)

## 225 Calibration approach

We used Bayesian inference to estimate the unknown parameters of the two ForClim regeneration models and their uncertainties. We estimated three species-specific ( $kL_{y,s}$ ,  $kDDMin_{y,s}$ , and  $kDrTol_{y,s}$ ) and two general ( $kEstDens$ ,  $kTrMax$ ) regeneration parameters of ForClim based on recruitment data from the EuFoRIa reserves. The species parameters were estimated for 11 out of 30 simulated species for which the data covered sufficient environmental variation. The species not  
230 considered for calibration were simulated with their default parameters (cf. Huber et al., 2020).

### Calibration target

The calibration target was to obtain recruitment rates in the model that match to observations. Tree recruitment was quantified as the number of trees that pass an inventory-specific DBH threshold. Observed decadal tree recruitment rates  $R_{i,s}$  were calculated for each plot  $i$  and species  $s$  with

$$R_{i,s} = \frac{\sum_{p=1}^{N_{periods}} R_{i,s,p}}{T_i \times 10}, \quad \text{eq. 8)}$$

235 where  $p$  is the inventory period and  $T_i$  is the total number of years between the first and the last inventory at plot  $i$ . Simulated tree recruitment rates  $\hat{R}$  were calculated as

$$\hat{R}_{i,s} = \frac{1}{N_{rep_i}} \sum_{k=1}^{N_{rep_i}} \frac{\sum_{p=1}^{N_{periods}} \sum_{j=1}^{N_{patch}_{i,s,p,k}} nTrs_{i,s,p,k,j}}{T_i \times 10}, \quad \text{eq. 9)}$$

where  $nTrs_{i,s,p,k,j}$  is the number of recruited trees for one patch  $j$ , inventory period  $p$ , and repetition  $k$ . Each simulation during the calibration was conducted on  $> 100$  patches (i.e., ca. 8 ha) to reduce the variability caused by the  $k$  stochastic realizations of the ForClim model. The trees in the initial forest inventory were randomly distributed to each of the 100 patches (each with  
240 a size of 0.08 ha) proportionally to actual plot size until a full repetition exceeded 100 patches. If one repetition was not a multiple of the patch size of 0.08 ha, the difference in exceeded plot area determined the proportion of additional trees drawn from all trees in the initial forest inventory to populate the patches. The number of repetitions  $N_{rep_i}$  for each plot  $i$  emerges from the next higher integer to  $\frac{8 \text{ ha}}{A_i}$ , where  $A_i$  is plot size in ha. This resulted in an average of 8 repetitions  $k$  across all sites, but with a range from plot sizes of 0.2 ha ( $k = 40$ ) to two sites with plot size  $> 4$  ha ( $k = 2$ ). The number of patches  $j$  ( $N_{patch}_{i,p,k}$ )  
245 within one repetition  $k$  is the next higher integer to  $\frac{100 \text{ patches}}{N_{rep_i}}$ .

### Model initialization

To initiate the calibration runs, we had to resolve the issue that trees below the inventory-specific DBH threshold (i.e., small trees), which may have been present in reality, are obviously not contained in the data. Ignoring these trees in the initialization

would create a temporal lag of tree recruitment (i.e., trees surpassing the DBH threshold), connected with a potentially  
 250 significant underrepresentation of tree regeneration directly after model initialization. To overcome this problem, we initialized  
 unobserved trees below the DBH threshold with the model's steady state (i.e., equilibrium of regeneration).

This steady state was determined by running the simulation with the stand structure of the initial forest inventory for 50 years,  
 suspending all processes affecting trees above or equal to the DBH threshold. During this "spin-up" phase, trees above the  
 DBH threshold that are included in the initial forest inventory could neither die nor grow, but still modulated the variables of  
 255 stand structure that affect regeneration (i.e.,  $gAL_0$ , Trs). In contrast, trees below the DBH threshold were allowed to grow and  
 die under the conditions observed in the initial inventory. If these newly regenerated trees grew larger than the DBH threshold  
 during the spin-up, they were removed. This means that these trees did not die from mechanisms that simulate tree mortality  
 in the model but were forcefully removed from the simulation to avoid the accumulation of trees with a DBH close to the DBH  
 threshold. Visual inspection of the simulation results showed that an equilibrium of the stand structure below the DBH  
 260 threshold was reached after approximately 50 simulation years, which was the reason to fix the spin-up to this time period.  
 After the spin-up, the simulation was continued with all trees and running all model processes (i.e., regeneration, growth and  
 mortality).

### Definition of goodness of fit

The goodness-of-fit was quantified by a (pseudo)-likelihood. We assumed that the observations  $R_{i,s}$  for site  $i$  and species  $s$   
 265 with the parameter vector  $\theta$  were negatively binomially distributed, leading to a log-likelihood per observation of

$$\log[P_s(R_{i,s} | \theta)] = \text{NegBinomial2}(R_{i,s} | \hat{R}_{i,s}, \phi). \quad \text{eq. 10}$$

Here, the mean  $\hat{R}_{i,s}$  is predicted by ForClim and governed by the calibrated values for  $kL_y$ ,  $kDDMin_y$ ,  $kDrTol_y$  and the  
 respective regeneration intensity parameter ( $kEstDens$  &  $kTrMax$ ) of the two models, as explained above, and the dispersion  
 parameter  $\phi$  of the negative binomial distribution, which can be interpreted as a measure of residual variation, is a free  
 parameter that needs to be estimated in addition to the model parameters.

270 We assumed that the dispersion may vary with species, DBH and plot size according to the formula

$$\phi = \phi_s \times e^{\phi_{DBH} \times DBH_i + \phi_A \times A_i}, \quad \text{eq. 11)$$

where  $\phi_s$  is the species-specific dispersion,  $\phi_{DBH}$  is the effect of the diameter threshold  $DBH_i$  and  $\phi_A$  the effect of plot size  
 $A_i$  on the dispersion. We used an exponential function to only allow for positive values, as required by the negative binomial  
 distribution.

The joint log-likelihood  $\log[P_s(y_s | \theta)]$  for each species  $s$  is the sum of the log-likelihoods over all plots  $i$  and species  $s$ :

$$\log [P(y | \theta)] = \frac{\sum_{s=1}^{N_{\text{species}}} \log [P_s(y_s | \theta)]}{N_{\text{species}}} \quad \text{eq. 12}$$

275 We additionally re-scaled the joint log-likelihood (eq.) by a factor of 1/12. The effect of this re-scaling is that uncertainties get wider and it reduces the absolute magnitude of (stochastic) likelihood differences. For both reasons, MCMC samplers are less prone to get stuck in local optima, whereas the shape of the posterior surface as well as posterior optimum remains unchanged. The re-scaling (which essentially corresponds to a down-weighting of the observational evidence by a factor of 12) can be interpreted as accounting for possible non-independence of the data and structural model error (see Oberpriller et al., 2021).

280 The choice of the value 1/12 was ad hoc, but given that some structural error and non-independence in the observations is likely present in this case, we believe the factor is in the right order of magnitude. Given the approximate nature of this correction, our scaled likelihood is more adequately described as pseudo-likelihood or an informal likelihood (Smith et al., 2008), and the same labels should be applied to the posterior. For this reason we use the term pseudo-likelihood whenever we refer to the measure of goodness of fit which was defined above.

285 In total, our pseudo-likelihood depends on a vector  $\theta$  consisting of 48 parameters, as we estimated three ecological threshold parameters ( $kL_y$ ,  $kDDMin_y$ , and  $kDrTol_y$ ; cf. Figure 1) and separate dispersion parameter  $\phi_s$  for each of the eleven species, plus one extra dispersion parameter for all other species, two parameters for the effect of DBH and plot area ( $\phi_{DBH}$  and  $\phi_A$ ), and one parameter for the regeneration intensity ( $kEstDens$  or  $kTrMax$ ) for the simple or the complex model, respectively. We defined wide uniform priors for each parameter that comprises the full range from the species' lowest and highest values in

290 the default parameterization in ForClim (cf. Table 1).

### Posterior estimation

We calibrated the model using the differential evolution sampler (DEzs, ter Braak & Vrugt, 2008) as implemented in the R Package *BayesianTools* (Hartig et al., 2019). We sampled with two independent sets of three chains (i.e., a total of six chains) for all 353 training plots. The z-matrix was re-initialized at the beginning of the sampling procedure (at 5000 to 6800 and 2000

295 to 3700 iterations for the simple model and the complex model, respectively) to improve the mixing of the chains. This was necessary because of the very wide prior range for the dispersion parameters, which led to a degenerated z-matrix. The same procedure was applied to improve mixing the chains after 120'000 to 139'300 (simple model) and 120'000 to 145'500 iterations (complex model). For the simple model, the upper prior range for the  $kEstDens$  parameter had to be adjusted from 0.02 to 0.2 after 139'300 iterations. Ultimately, after 191'600 (simple model) and 200'900 iterations (complex model), one set

300 of three independent chains converged, as judged by the visual inspection of the chains and Gelman and Rubin's MCMC Convergence Diagnostic (cf. Table A4). The other set of independent chains did not fully converge, mostly because of one chain being stuck for the species-specific dispersion parameters. Computational constraints did not allow for running the sampler even longer. One single simulation took 3 seconds per plot, i.e., 6 chains times 353 calibration plots resulted in a total computation time of 1.765 h per iteration without parallelization. Fortunately, the Euler High Performance Computing Cluster

305 of ETH Zürich enabled us to use 1000 cores (500 per model variant) and sufficient memory. The effective computing time, including the overhead when utilizing all resources, was 10-15 seconds per iteration and ca. 25 days in total for each model variant.

The posterior distribution from the calibration consisted of 1'000 samples drawn from the last 32'300 (simple model) and 45'400 iterations (complex model). The simulations from the posterior parameter distribution provided posterior estimates of  
310 decadal tree recruitment rates ( $\widehat{R}_{i,s}$ ) for all 343 test plots  $i$  and species  $s$ . The Mean Posterior Estimate (MPE) and the 80% Credible Intervals (CIs) of  $\widehat{R}_{i,s}$  from the 1'000 posterior simulations were used to assess residuals and evaluate model performance (see Table A4). The MPE and CIs for the parameter estimate of the posterior distribution were used to compare the trait based model and the calibrated model.

### **Performance comparison using Root mean squared error (RMSE) and marginal pseudo-likelihood (ML)**

315 Model performance was assessed with the root mean squared error (RMSE) and the marginal pseudo-likelihood (ML) on both training and hold-out data. The difference between the two metrics is that RMSE is a general metric of fit, while the marginal pseudo-likelihood is Bayesian metric that relates to the Bayes Factor and posterior model weights and thus allows to compare the support for two alternative models based on a specific likelihood.

For the simulations from the calibrated and trait-based models the RMSE was calculated for different DBH thresholds: for  
320 variable thresholds between plots and harmonized DBH thresholds of 7 and 10 cm. This harmonization was done by artificially increasing the DBH threshold in the observed and simulated data to mimic a consistent inventory design with a common DBH threshold. We calculated the RMSE from the training and test data based on the comparison of observed and simulated recruitment across the species-unspecific, the species-specific, and as the average over the species-unspecific and species-specific RMSEs (Table 2).

325 The ML was calculated for the simulations from the calibrated models only because the pseudo-likelihood relies on the dispersion parameters, which were not estimated for the trait based model. The ML is the average pseudo-likelihood of the model given the training or the test data, averaged over the posterior parameter uncertainty (cf. Delpierre et al., 2019). We evaluated the ML in both cases on the validation data based on the posterior distribution inferred from the training data. This approach, which corresponds to the fractional Bayes factor (O'Hagan, 1995), avoids inconsistencies when comparing models  
330 with weak or uninformative priors. The Bayes Factor is then obtained by taking the ratio between two marginal likelihoods with  $e^{M1-M2}$ . This provides the relative posterior support of M1/M2 by the data (Kass and Raftery, 1995).

When interpreting the results, it is important to remember that both RMSE and ML as evaluated here will typically be higher for more complex models on the training data, so the comparison of models with these metrics on the training data is of limited use. However, models can sensibly be compared by their performance on the hold-out, and it is also informative to look at the  
335 reduction of performance between training and hold-out, which gives an indication of overfitting.

## Posterior sensitivity

Global sensitivity analyses allow for the assessment of model behavior across large parameter spaces. However, large parameter spaces may also cover unrealistic parameter configurations, and computational requirements are high. Therefore, a strategy for constraining the parameter space to a relevant location is required (cf. Huber et al., 2018). We combined the  
340 benefits of a global and a local sensitivity analysis by constraining the parameter space via deriving a posterior distribution from the observations. This allowed us to evaluate model sensitivity with respect to the uncertainty derived from observed recruitment patterns in European forest reserves.

To analyze the sensitivity of regeneration to changes in the model parameters within the posterior distribution, we analyzed the effect of increased tolerance of trait values (i.e., lower  $kL_y$ , higher  $kDrTol_y$ , and lower  $kDDMin_y$ ) on simulated recruitment  
345 within the posterior parameter range. This was done by modeling  $\hat{R}$  with a GLM and a negative binomial distribution with z-scaled values of negative  $kL_y$ , negative  $kDDMin_y$ , and positive  $kDrTol_y$  as predictors. This model was implemented using glmmTMB (Brooks et al., 2017).

## Results

### Species traits and regeneration intensity

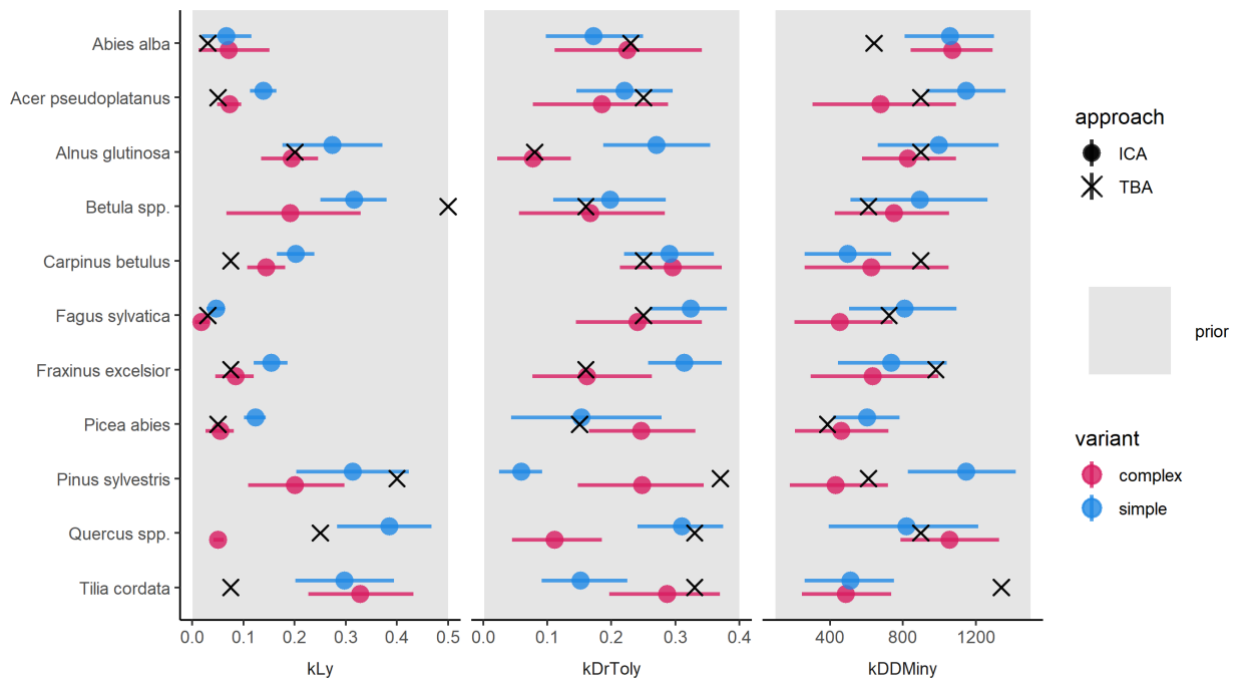
350 The trait-based regeneration niche differs from the regeneration niche that emerges from the model which was calibrated with the observations in unmanaged forest reserves. Variation in these differences is evident between trait types, species, and model variants (Figure 2 and Table A2).

Light requirements stand out from the other traits because they were most sensitive during model calibration, as indicated by the narrow posterior distributions compared to the prior parameter range (Figure 2, left and Figure A2a). Most posterior  
355 estimates were not only narrow, but also supported by the trait values (Figure 3, left). Estimates of the complex model were generally closer to the trait values, with a good rank correlation (i.e., Spearman's  $\rho = 0.57$ ). Light requirements defined by traits for the simple model were systematically lower compared to the values emerging from the calibration. Nevertheless, a Spearman's  $\rho$  of 0.94 indicates that the calibration put the species in a plausible order (Figure 3, top left). The estimates of the species-specific light requirements were more similar between both approaches for shade-tolerant tree species in general.  
360 Values from the calibration for *Quercus* spp., *Pinus sylvestris*, and *Betula* spp. were much lower compared to the trait values in the complex model but more similar in the simple model. For *Tilia cordata*, the calibration led to much higher light requirements compared to the trait based values with either model (cf. Figure 2, left).

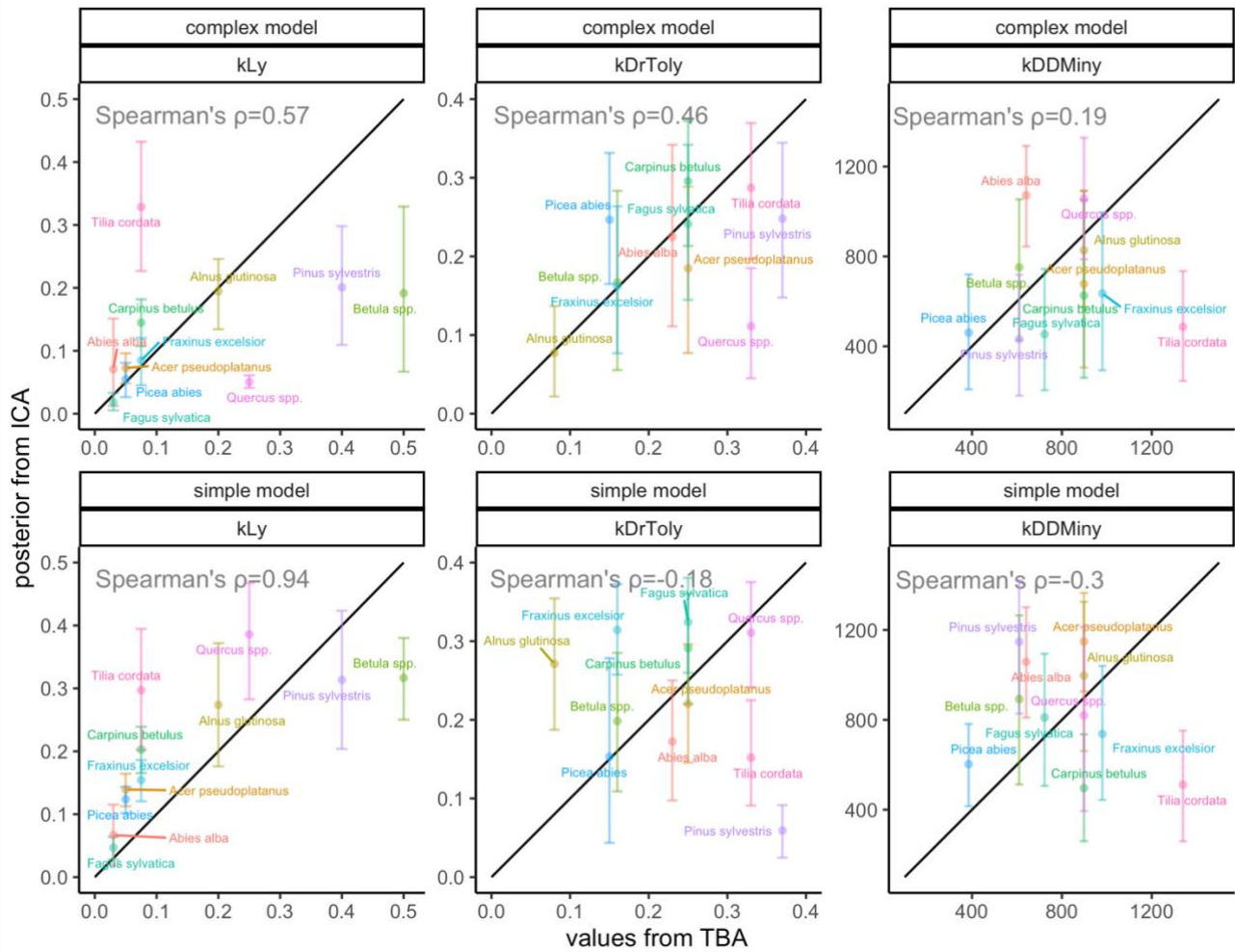
Drought tolerance values from both approaches' matched moderately well when using the complex model (Spearman's  $\rho = 0.46$ ) with relatively large CI, and the expectation was within the CI for eight species (Figure 2, center). The MPE from the  
365 calibration was close to the definitions of the trait values for five species. However, drought tolerance estimates from the calibration did not match the trait values well for the simple model (Spearman's  $\rho = -0.18$ ). Only for six species the wide

370 CIs included the trait based values, and the MPE matched the trait values in the simple model for two species only. For *Quercus* spp. (complex model), *Tilia cordata* (simple model) and *Pinus sylvestris* (both models), the calibration led to much lower values compared to the trait values. Conversely, for *Alnus glutinosa* and *Fraxinus excelsior* the calibration resulted in higher values compared to the trait-based values (cf. Figure 2, center).

375 Estimates for the minimum degree-days had wide CI for both models and a low rank correlation between the approaches (Spearman's rho = 0.19 for the complex model and -0.3 for the simple model; Figure 2, right). Although the posterior CI of the calibration included the trait-based values for many species, the intervals were wide and the MPE values were close to the trait-based values only for two and three species in the complex and simple model, respectively. This indicates that the calibration values neither fully disagree nor perfectly match the trait-based values. For *Tilia cordata* (both models) and *Carpinus betulus* (simple model), the calibrated values were much lower compared to the trait-based values. Conversely, the calibrated degree-day values for *Pinus sylvestris* (simple model) and *Abies alba* (both models) were considerably lower compared to the trait-based values (cf. Figure 2, right).



380 **Figure 2: Mean Posterior Estimate including the 80 % CI of the species-specific parameters for the complex (red) and the simple model (blue). Point type indicates the inverse calibration approach (ICA) and the trait-based approach (TBA). The panels show the species trait values light requirements (*kL<sub>y</sub>*), drought tolerance (*kDrToly*), and minimum degree-days (*kDDMinLy*). The uniform prior parameter range (min, max) of each species trait (x-axis) is indicated by the grey rectangle in the background.**



385 **Figure 3: Comparison of expected values for species-specific establishment thresholds based on ecological knowledge (TBA, trait-based approach; cf. Leuschner and Ellenberg, 2017) and MPE (ICA, inverse calibration approach, this study). The range displays the 80 % CI for the complex (top panels) and the simple model (bottom panels). The 1:1 relationship is indicated by the black line. Spearman's rank correlation and the p-values of the MPE and the trait-based approach (TBA) values are shown in each panel.**

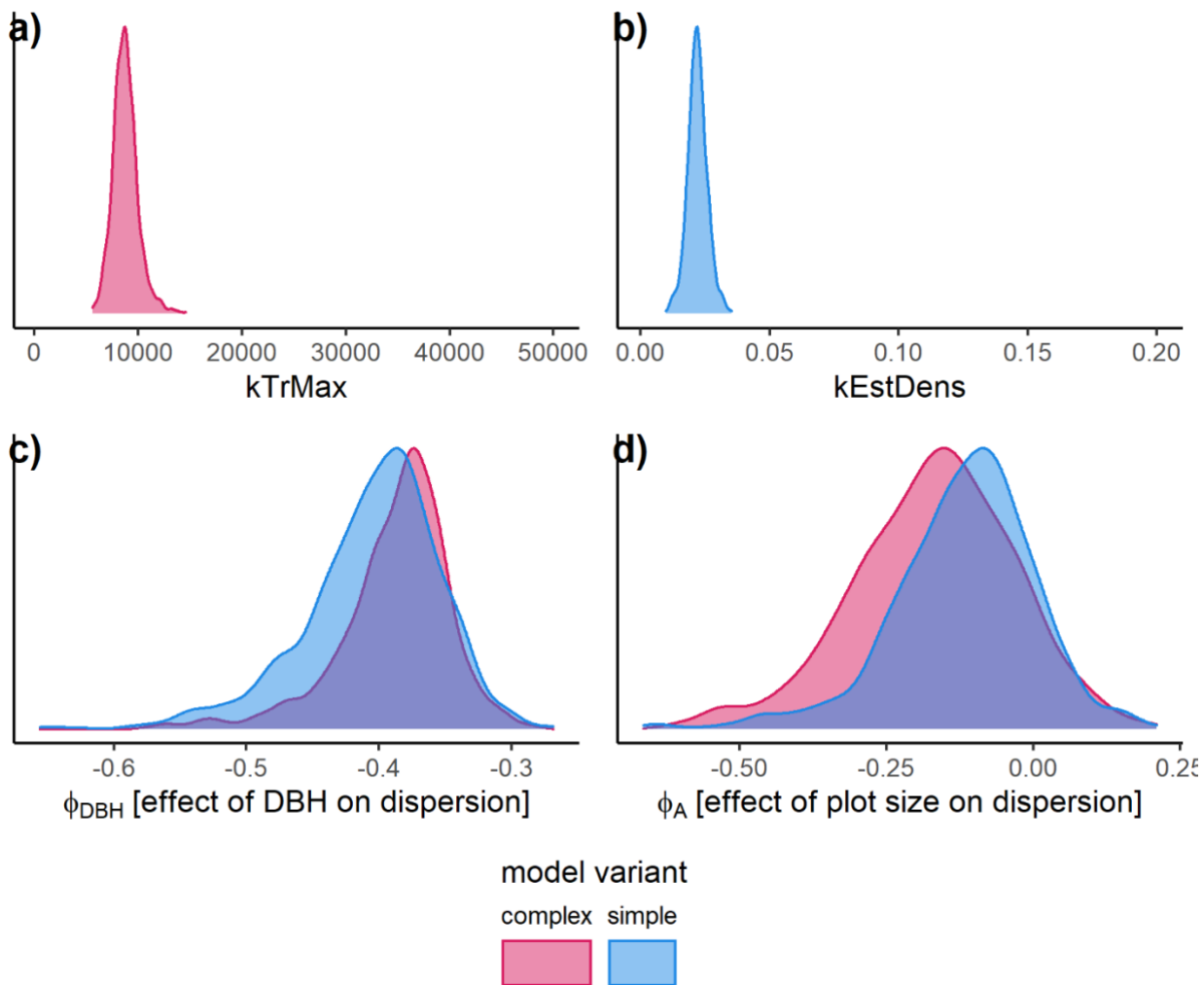
The estimates of the calibration for general regeneration intensity were narrow compared to the prior (Figure 4) and therefore considerably sensitive. While the species-unspecific parameter kTrMax from the calibration (complex model) was significantly lower than its default value of the trait-based model, the species-specific parameter kEstDens (simple) was higher than its default value of the trait-based model (Table A1). Considering the interaction between kEstP (which was reduced by a factor of 1/5) and kEstDens or kTrMax (cf. model description in Appendix B), the overall amount of regeneration is generally lower for the calibrated model compared to the trait-based model. Specifically, for the complex model the MPE (kTrMax = 8762) suggests 25 times less maximum regeneration compared to the default values of the trait-based models (kTrMax = 50000 · 5 = 250000); and for the simple model the MPA (kEstDens = 0.022) suggests a reduction of ca. 24 % per species compared to

390

395

the default trait-based model ( $kEstDens = 0.006 \cdot 5 = 0.03$ ). However, it is noteworthy that these parameters modulate regeneration differently and the magnitude of the deviation between the parameters in the calibrated model, the default trait-based model, and the model variants is not directly translated into the simulated regeneration amount within the model (cf. Figure 1 and the full set of equations in Appendix B).

The coefficient for the effect of the DBH threshold in the species-specific dispersion was significantly different from zero, with an MPE of -0.39 and -0.41 for the complex and simple model, respectively. This indicates that dispersion increases for higher DBH thresholds (Figure 4c). The coefficient for the effect of plot size is slightly negative but not significantly different from zero (Figure 4d), which indicates that there is no significant effect of plot size on dispersion. However, a very weak positive effect of larger plots on dispersion is visible. On the species level, dispersion effects differed significantly, with the lowest dispersion for *Fagus sylvatica* and the highest for *Quercus* spp. (Figure A1 and Table A3). These findings emerged from both the simple and the complex model (cf. Figure 4 c and d).



410 **Figure 4: Posterior distribution of the non-species specific parameters determining the amount of regeneration: a) kTrMax (complex model, red) and b) kEstDens (simple model, blue). Effects on the dispersion parameter  $\phi$ : c) DBH threshold and d) plot size. The prior parameter in a) and b) is given by the extent of the graph. The prior range for the dispersion parameters was -5 to 5 and is not shown. Note that lower values of the dispersion parameter indicate higher dispersion. Consequently, negative estimates for dispersion are positive effects on the actual dispersion. Species' dispersion parameters are presented in Table A3.**

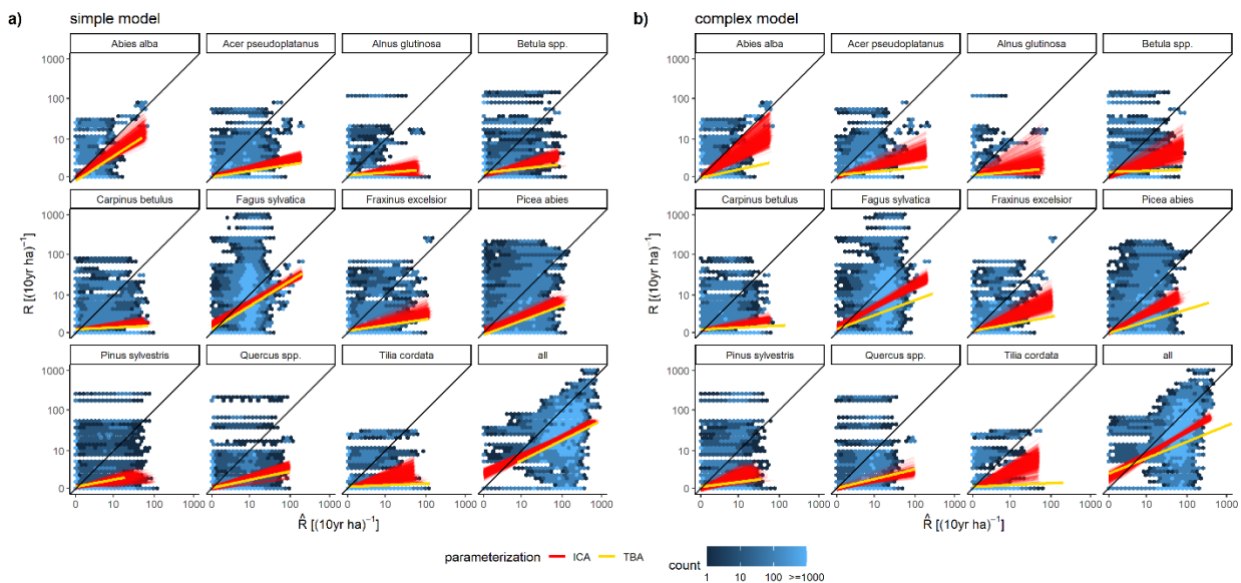
### Model performance

415 The calibration led to somewhat better performance compared to the trait-based approach (Figure 5 and Table 2). Both model variants performed better when calibrated and revealed the uncertainty of the posterior simulations. However, performance differed strongly between species. Most gains in performance coupled with a high degree of uncertainty were evident for *Abies alba* and *Tilia cordata* with both models (Figure 5). No increase in performance was evident for *Quercus* spp. and *Alnus glutinosa*, although high uncertainty of the simulations was evident for *Alnus glutinosa* with the complex model. Slight but  
 420 distinct gains in performance were found for *Fagus sylvatica* and *Picea abies* with the complex model. Note that not only the intercept for the comparison of observations and simulations changed, but also the slope, which indicates that this was not only due to the regeneration intensity parameters. Overall performance increased distinctly for the complex model, and considerably for the simple model (cf. RMSE in Table 2). In summary, the calibration clearly improved model performance for almost all species in the complex model and to a limited extent in the simple model. In addition, the uncertainty based on the posterior  
 425 parameter distribution was clearly visible in the simulations. The RMSE decreased with increasing DBH threshold (Figure A3) for both models.

The ML confirmed the higher performance of the complex model (ML = -391.61) compared to the simple model (ML = -401.86), which was also evident from the RMSE (Table 2 and Figure A2b). According to Kass and Raftery (1995), the Bayes Factor from the training data being above 200 suggested strong support for the complex model (Bayes Factor = 28282.54).

430 **Table 2: RMSE of simulated and predicted R and pseudo-likelihood for the different models and approaches: inverse calibration approach (ICA); trait-based approach (TBA). The marginal pseudo-likelihood (ML) was derived from the posterior parameter distribution of the training data (N=353), and the test data (N=343). Species specific RMSE values are presented in Figure A4.**

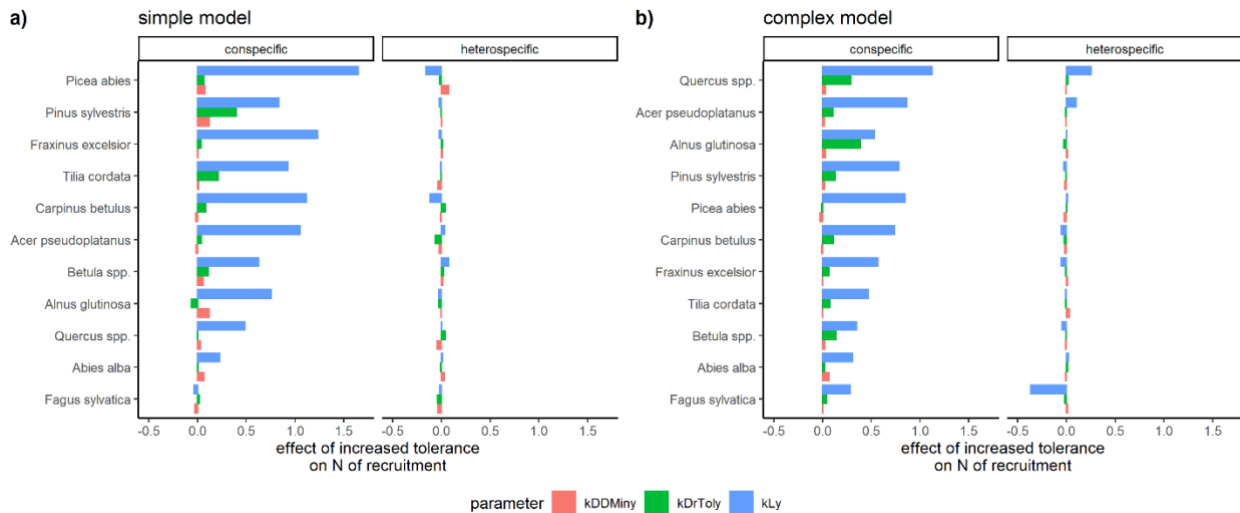
	complex				simple			
	ICA		TBA		ICA		TBA	
	test	training	test	training	test	training	test	training
RMSE	5.84	6.19	8.86	9.29	6.32	6.63	6.17	6.47
ML	-391.61	-411.38			-401.86	-419.65		



435 **Figure 5: Simulated vs. observed recruitment rates at 7 cm DBH of the 11 species for (a) the simple and (b) the complex model. The red lines show linear regressions from 1000 simulated recruitment rates using the posterior parameter distribution at the 343 test plots. The data points used for the regression are indicated by the blue color of the hexagons, where light blue indicates fewer points and dark blue indicates more points. The yellow lines are characterizing the recruitment rates for the same test plots based on the default parameter setting (TBA, trait-based approach).**

#### 440 **Posterior sensitivity**

The variation of the parameter values characterizing the species' light requirements had the strongest effect on conspecific regeneration for either model variant (Figure 6 a and b, respectively). The variation of drought tolerance within the posterior, which was rather high, had a much weaker effect on conspecific recruitment, and the minimum degree-days had a very low effect on recruitment within the posterior parameter range. Interestingly, positive effects for heterospecific recruitment were evident in the case of higher shade tolerance of *Quercus* spp. and *Acer pseudoplatanus*, but only in the complex model (Figure 6b). *Picea abies* (simple model) and *Fagus sylvatica* (complex model) showed the strongest negative effects on the emergence of heterospecific recruitment (Figure 6).



450 **Figure 6: Estimates of the effect of increased tolerances for  $kL_y$ ,  $kDrToly_y$ , and  $kDDMin_y$  on the emergence of conspecific and heterospecific recruitment for the simple (a) and the complex model (b). The effect sizes correspond to the coefficients from a GLM that predicts recruitment with scaled tolerance parameters so that they have a mean of 0 and a standard deviation of 2; an increase of the value always indicates an improvement for the species.**

## Discussion

Below, we discuss the research questions with respect to the results and the ecological implications of our findings. First, we focus on the differences of the species-specific traits between the calibrated and the trait-based model; second, we evaluate how the structure of the simple and complex model affected performance; and third, we discuss technical advances and methodological aspects.

## Species traits

The species trait values varied considerably between the calibrated models, the trait based-models, and the two model variants. We aim to explain these differences by reflecting on a) the theoretical expectations of the two approaches, and b) the structural differences between the model variants.

Differences between the trait-based and calibrated models can be expected based on ecological considerations regarding the regeneration niche (Grubb, 1977) and ontogenetic niche shifts (Werner and Gilliam, 1984), as well as methodological aspects such as the importance of context for modeling trait-demography relationships (Yang et al., 2018). Specifically, we expected high sensitivity and a good match for the shade tolerance of the species because light availability is a key determinant of tree regeneration on small spatial scales (Collins and Good, 1987), and its context is modeled explicitly and in rather high detail in ForClim (cf. the direct link between stand structure and light availability in equations eq. 1 to eq. 3). In contrast, the context of trait values related to climate (drought tolerance and temperature requirements) is only vaguely defined by species distribution limits (Meusel et al., 1965) along macroclimatic gradients (Rudloff, 1981). In addition, the traits for light

470 requirements are differentiated between juveniles and adults (Leuschner and Ellenberg, 2017), while those related to climate are not. Therefore, we expected less agreement between the calibrated and trait-based models for these latter drivers. Our results supported these expectations, as shown by the mostly good agreement between the light requirement parameters compared to climatic parameters in the two approaches. Notably, this pattern was found in both the simple and the complex model, and it thus appears to be a robust feature irrespective of the structure of the regeneration model. Furthermore, the  
475 drought-related parameters matched better between the calibrated and the trait-based models in the complex variant, which indicates that trait values embedded in a model that connects drought effects and competition during regeneration have more support by the data. This interlink of competition and drought has also been demonstrated in grassland communities (Grant et al., 2014; Levine et al., 2022) and tree species mixtures (Jucker et al., 2014; Grossiord, 2020; Young et al., 2017; Clark et al., 2016; Ruiz-Benito et al., 2013; Haberstroh and Werner, 2022).

#### 480 **Light**

The nuanced differences between the model variants in terms of the estimates of the species' light requirements can be put in context with the regeneration intensity parameter. The calibrated trait values from the complex model were almost identical for most species to the trait-based values (Larcher, 1996; Lyr et al., 1992), whereas in the simple model the light requirements were systematically lower in the calibrated compared to the trait-based models. This indicates that in the simple model,  
485 excessive recruitment levels (as embodied in the parameter *kEstDens*) were compensated for by erroneous light requirements (cf. Figure 2). These inconsistencies may arise from the structure of the simple model, where the amount of recruitment is equal for all species that regenerate. Thus, the simple model lacks flexibility to a) generate an appropriate number of recruits for the dominant species and b) lower the number of recruits for less dominant species. This explanation is supported by two other findings: the estimates of light requirements for the often-dominant species *Fagus sylvatica* matched the trait-based  
490 values, while almost all other species had exaggerated estimates (Figure 2); and the sensitivity of *Fagus sylvatica* to light within the posterior distribution was close to zero, with considerable uncertainty regarding the modulating effects of light for other species (Figure 6). The light-demanding tree species *Quercus* spp., *Pinus sylvestris* and *Betula* spp. along with *Tilia cordata* did not match expectations either, which is in line with this pattern. These findings suggest that structural problems regarding competition for light in regeneration models of European forests can be exposed by the behavior of *Fagus sylvatica*.  
495 Thus, if the competitive dominance of *Fagus sylvatica* is not captured appropriately, a calibrated model is likely to compensate this elsewhere.

In contrast to the absolute values for light requirements, their ranking of the species was more similar between the approaches for the simple model (Figure 3). The lower rank correlation of the complex model is mostly due to much lower estimates for light demanding tree species such as *Betula* spp., *Pinus sylvestris*, and *Quercus* spp., thus suggesting that the simple model  
500 performs better in simulating regeneration of early successional species. One possible reason for this behavior could be that all establishment factors (i.e., environmental drivers of regeneration) are assumed to be equally important in virtually all vegetation models, including ForClim (cf. Bugmann & Seidl 2022). This assumption has different implications for a model with competition between species (complex model) compared to a model without competition (simple model). This becomes

clear if we consider a stand with high light availability. Then, the light requirements of all species are fulfilled. Within the simple model, the species establishment count takes into account their successional strategy, while the complex model lacks this mechanism and may favor species with higher suitability derived from factors other than light, thus blurring the overwhelming effect of the life-history strategies on the amount of tree regeneration under high light conditions (cf. Welden and Slauson, 1986). Subsequently, the simple model adjusts excessive regeneration by the processes of growth and mortality. By contrast, in the complex model there may be too few early successional trees, and subsequent compensation is insufficient. This notion is supported by the fact that RMSE decreased with higher DBH thresholds and suggests that unrealistic regeneration patterns must be compensated in vegetation models by subsequent growth and mortality (cf. Díaz-Yáñez et al., in press)

In summary, the light niche of most species was recovered considerably well. If the identified inconsistencies regarding light requirements are caused by structural problems of the model, our results provide strong support for the quantification and ranking of species' trait based light requirements (i.e., the original parameterization of species light requirements in ForClim).

### **Drought**

The credible intervals (CIs) of the estimates for drought tolerance were wide in the calibration for both model variants, and for the complex model the rank correlation between calibrated and trait-based values was better. The ranking of species trait-based drought tolerance values is ecologically plausible and widely accepted (Huber et al., 2020; Bugmann, 1994; Leuschner and Ellenberg, 2017). Yet, a key difference between the structure of the simple and complex model is competition during regeneration, which may explain the better rank correlation for the complex model (cf. Grant et al., 2014; Andivia et al., 2018; Käber et al., 2023a). However, the CIs of the calibration estimates were high, and various mismatches were evident. We surmise that they arise from an oversimplified representation of drought where nuanced differences between species drought tolerances and potential facilitation effects are not reflected (Lortie and Callaway, 2006). A different and more detailed perspective on modeling competition for drought is considering the intra- or interannual variability of water availability in contrast to species phenological requirements (cf. Detto et al., 2022 and Levine et al., 2022). However, mismatches in temporal and spatial scales between the representation of drought in the simulations and actual drought conditions at the observed sites, coupled with errors in the input variables (climate and soil properties), and observations are possible reasons for high CIs (cf. Shoemaker et al., 2020). Consequently, we would expect higher predictive ability of tree species traits for drought on smaller scales with clearly defined relations between environmental drivers and outcomes, as shown by Li et al. (2022), who found that species traits explained more variation in tree seedling performance under controlled conditions in experiments compared to large-scale studies (cf. Paine et al., 2015). For the simple model, the estimates did not follow a clear pattern, and it is difficult to assess whether the estimates that are close to the expectation (e.g., for *Picea abies*) are actually providing signal, or are just random. Despite these uncertainties, it is noteworthy that some species-specific trait-based values were recovered with the calibration, thus providing at least some support by the calibrated drought-related regeneration niche as it was defined by the traits.

## Temperature

In contrast to the two other autecological parameters, the calibration estimates for the minimum degree-day requirements rarely matched the trait-based values. In general, the species minimum degree-days had wide CIs. We consider three factors to explain this. First, the manifold effects of temperature on regeneration at different scales, which cannot reasonably be aggregated into one single parameter, coupled with the fact that the original source of the trait values did not differentiate juvenile distribution ranges (Meusel et al., 1965; Kienast, 1987; Rudloff, 1981). Second, ontogenetic shifts (e.g., Vitasse, 2013) and demographic dependencies, i.e., the cumulated survival probability and growth over a tree's lifetime (cf., Grubb, 1977; Heiland et al., 2022). And third, it is likely that temperature-related processes are limiting regeneration much less often in our data set compared to the persistent and strongly varying competition for light (cf. Grime and Mackey, 2002; Vincent and Harja, 2008). Distinguishing between filters for the macroclimatic factors along with dynamic small-scale filters might be a better conceptual basis for more realistic and more accurate tree regeneration models (but see Thakur and Wright, 2017). Consequently, with respect to process formulations in dynamic models, valid growth and mortality formulations might be more important for temperature-regeneration relations than the formulation of the initiation phase of tree regeneration.

## 550 Model performance

Generally, the calibration resulted in much better performance for the complex and a moderate improvement for the simple model compared to the trait-based approach. This is consistent with previous studies using Bayesian calibration of dynamic models (Augustynczyk et al., 2017; Cailleret et al., 2019; Trotsiuk et al., 2020; Van Oijen et al., 2005). The main reason for this improvement in both model variants is the overall lower regeneration amount, which results from the combination of establishment probability and regeneration intensity. Thus, our results suggest that calibration can help to sharpen the estimates of regeneration parameters that are not well-constrained by standard empirical data.

The somewhat better performance of the complex model is best explained by the way the species-specific amount of regeneration is determined. While the simple model does this uniformly, the complex model distributes the regeneration to the species according to their environmental suitability. This is also reflected in the more realistic estimates of the regeneration niche along the drought gradient. Overall, our findings corroborate the considerations of Huber et al. (2020), who suggested the simultaneous use of different model variants. In our study, the regeneration patterns across the very heterogeneous forest types in our data set was captured much better by the complex model, which implicitly allows for differentiating processes (captured via the EFs) in the regeneration layer. In contrast, the ideas underlying the simple regeneration model, which was originally developed for multi-species forests with high evenness (Botkin et al., 1972), turned out to be less suitable for reproducing the observed regeneration patterns.

In addition to established performance measures such as RMSE or the Bayes Factor, the comparison of the default trait values and inversely calibrated trait values allowed us to evaluate whether the calibrated parameters are just 'degrees of freedom' that are used to make the model fit better to the data, or whether their estimates are plausible from an ecological perspective (cf.

Hellegers et al., 2020). Based on the discussion on species trait values above, this leads to the conclusion that the simple model  
570 is more realistic for the factor light, whereas the complex model captures processes related to drought better.

## **Methodological considerations**

### **Spin-up phase**

We used a spin-up phase for dealing with the lack of information on small trees (i.e., the trees that are smaller than the diameter  
threshold, which inevitably has to be used in any inventory) in the initial state of the forest inventory. The spin-up phase proved  
575 to be a good solution because regeneration amounts were generally in agreement with observations. However, we were unable  
to evaluate whether the assumption of a steady state of regeneration below the DBH threshold was realistic. For this, data with  
much higher temporal resolution and a low DBH threshold ( $\leq 1.27$  cm) would be necessary. Theoretically, our approach would  
lead to biased regeneration if actual conditions for regeneration are significantly different from the conditions observed in the  
initial inventory. For example, lower light availability in the actual conditions would lead to a bias towards shade intolerant  
580 species, conversely higher light availability would lead to a bias towards shade tolerant species. In addition, the overall  
regeneration amount could be affected by these biases. Thus, we encourage future studies to test the implications of our  
assumptions to evaluate potential bias introduced by our approach.

### **Dispersion**

Processes that are not considered in the models could explain further variation of parameters and performance between  
585 approaches and model variants. We found that the dispersion parameter of the negative binomial distribution was mostly  
determined by ecological processes: large differences of dispersion between species indicate that species-specific factors play  
a key role, as discussed below.

One such factor is the regeneration strategy, for which light requirements usually are a good predictor (Grime, 1977). Species  
with high light requirements that require disturbances for regeneration (e.g., *Betula* spp., *Pinus sylvestris*) featured higher  
590 dispersion than typical late-successional, shade-tolerant species (e.g., *Fagus sylvatica* or *Picea abies*). This pattern was also  
reflected for intermediate species on a gradient from low to high light requirements. However, not all species follow this  
pattern.

Migration limitations are another factor that are likely to contribute to species-specific range limits. Specifically, the range  
limits of *Abies alba*, *Carpinus betulus*, and *Quercus* spp. are potentially determined by lags in postglacial range expansion  
595 (Mauri et al., 2022; Svenning et al., 2008) and its interplay with long-term demographic processes and competition (Scherrer  
et al., 2020). The mismatch between estimated and ecologically plausible parameters could be caused by the model assumption  
that seeds of all species are available all the time, and the associated absence of dispersal limitations in the model. Dispersion  
parameters that are based on real-world observations account for such problems when using likelihood-based approaches for  
model evaluation. Consequently, species-specific clustering (e.g., random draws from a negative binomial distribution) could  
600 substitute mechanisms that are not explicitly included in dynamic forest models. However, the parameterization of such

mechanisms would be challenging because it would require a process-based justification, otherwise dispersion parameters are only useful as a statistical measure for clustering in observed data (Hartig et al., 2012).

Overall, whether the incorporation of dispersion is beneficial in a model calibration study depends on the purpose of the study. For achieving higher accuracy of stand-level predictions, our study demonstrates that dispersion must be accommodated.

605 Especially validation and calibration studies require dispersion components to enable a reliable comparison of simulations with observations of tree regeneration. From a theoretical point of view, however, the incorporation of dispersion is not necessarily required. For example, a study on different management scenarios without considering dispersion can still generate valuable insights for silvicultural decisions if the assumptions and context are clearly defined.

### **Pseudo-likelihood**

610 Our approach to derive the likelihood (cf. eq. 8 to 12) proved to be generally useful for our model calibration. Nevertheless, several aspects regarding the approach applied here can be improved in follow-up research. First, we deal with a stochastic likelihood that makes it extremely difficult for the DEzs sampler to efficiently sample the parameter space. We acknowledge that theoretically other approaches such as Bayesian Synthetic Likelihood (Wood, 2010) or Approximate Bayesian Computation (Csilléry et al., 2010) might solve the issue of intractable likelihoods more elegantly than our approach. However, 615 computation time would be a major challenge if one wanted to apply these alternative approaches. Second, we focused on decadal average tree recruitment rates as a benchmark for evaluating the tree regeneration niche. This aggregates over many subprocesses and does not explicitly include the factor time in the pseudo-likelihood. We did not consider early growth or mortality just after establishment either. Future studies may consider all three demographic processes simultaneously to construct an improved benchmark of model accuracy (Bröcker and Smith, 2007; Dietze, 2017). Third, our study covered only 620 very few boreal plots, and rarely the transition towards very dry, Mediterranean-type forest ecosystems. Thus, future studies could benefit strongly from extending the environmental gradients to more extreme climates, so as to reduce parameter uncertainty. Thus, our study also underlines the importance of long-term monitoring of forest ecosystems over a wide range of conditions (cf. Hanbury-Brown et al., 2022).

### **Conclusion**

625 This study aimed to compare two tree regeneration models of different complexity and to examine their ability in capturing the regeneration niche of eleven tree species in unmanaged European forests. Furthermore, we sought to gain a deeper understanding of the effectiveness of two approaches to parameterize tree regeneration in dynamic forest models.

The comparison of the regeneration niche emerging from the inverse calibration approach and the predefined niche of the trait-based approach revealed that calibration led to better predictions of tree regeneration. The improvements were mostly caused 630 by the lower regeneration intensity compared to the trait-based models. Decreases in regeneration intensity were modulated by competition for light with a subordinate role of drought. Temperature was not sensitive, and based on the EuFoRIa dataset it was not possible to recover the temperature-based niche. The mismatches between predefined and inversely calibrated trait values led to the conclusion that competition for light is the key processes for tree regeneration along with parameters that

modulate tree regeneration amount. We therefore hypothesize that climatic drivers must become more important after initial  
635 establishment, having pronounced effects on tree growth and, indirectly, on mortality.

Furthermore, we found that a more complex model that incorporates competition during regeneration features a higher performance compared to a simple model without competition. This highlights the importance of considering the interactions between species during the regeneration process and underscores the potential of adding model complexity for improving model performance.

640 Future research faces the challenge of identifying the sweet spot between simulating realistic, nuanced regeneration amounts for individual species on the one hand and excessive regeneration that must be regulated later in tree life by growth and mortality on the other hand. While the former might expose more structural problems of the model with the consequence of unrealistic species composition and insufficient regeneration intensity, the latter potentially results in overoptimistic predictions of forests regenerative capabilities, with consequences e.g. for the assessment of the adaptive capacity of forests  
645 to climate change.

Overall, we encourage the use of inverse calibration to improve the understanding of the relation of real-world observations and tree regeneration models. Our major contribution to improve tree regeneration models lies in the finding that overall regeneration intensity and light availability are the most important factors that govern tree regeneration. Conversely, macroclimatic drivers (i.e., effects of climate) are not expected to directly alter the emergence of small trees but rather affect  
650 tree regeneration by modulating the light availability via increased mortality of larger trees. Thus, the accuracy of predictions of tree regeneration for the resilience of forests under climate change may depend more strongly on the representation of within-stand dynamics than the species range limits along large climatic gradients.

### **Code and data availability**

The current version of *model* is available from the project website: <https://ites-fe.ethz.ch/openaccess/products/forcclim> under  
655 the GNU GENERAL PUBLIC LICENSE v3. The exact version of ForClim used to produce the results used in this paper is archived on Zenodo (<https://doi.org/10.5281/zenodo.8334092>), as are input data and scripts to run the model and produce the plots for all the simulations presented in this paper (<https://doi.org/10.5281/zenodo.8334092>).

### **Acknowledgements**

We thank all researchers of the European Forest Reserves Initiative (EuFoRIa, [www.euforia-project.org](http://www.euforia-project.org)) who contributed  
660 long-term data for this study. EuFoRIa has been invaluable for this study, and we are grateful for their support and trust. In particular we thank Thomas A. Nagel (University of Ljubljana, Ljubljana, Slovenia), Tuomas Aakala (University of Eastern Finland, Joensuu, Finland), Markus Blaschke (Bavarian State Institute for Forestry, Freising, Germany), Bogdan Brzeziecki (Warsaw University of Life Sciences, Warszawa, Poland), Marco Carrer (University of Padova, Legnaro, Italy), Eugenie

Cateau (Reserves Naturelles de France, Quetigny, France), Georg Frank (Austrian Federal Research Centre for Forests, Natural Hazards and Landscape (BFW), Wien, Austria), Shawn Fraver (School of Forest Resources, University of Maine, Orono, Maine, USA), Jan Holik (Silva Tarouca Research Institute, Brno, Czech Republic), Stanislav Kucbel (Department of Silviculture, Faculty of Forestry, Technical University Zvolen, Slovakia), Anja Leyman (Research Institute for Nature and Forest, Brussels, Belgium), Peter Meyer (Northwest German Forest Research Institute, Göttingen, Germany), Renzo Motta (University of Torino, Torino, Italy), Pavel Samonil (Silva Tarouca Research Institute, Brno, Czech Republic), Lucia Seebach (Forest Research Institute of Baden-Württemberg, Freiburg, Germany), Jonas Stillhard (Swiss Federal Institute for Forest, Snow and Landscape Research, Birmensdorf, Switzerland), Miroslav Svoboda (Czech University of Life Sciences, Prague, Czech Republic), Jerzy Szwagrzyk (University of Agriculture, Krakow, Poland), Kris Vandekerhove (Research Institute for Nature and Forest, Brussels, Belgium), Ondrej Vostarek (Czech University of Life Sciences, Prague, Czech Republic), Kamil Kral (Czech University of Life Sciences, Prague, Czech Republic), Tzvetan Zlatanov (Institute of Biodiversity and Ecosystem Research, Bulgarian Academy of Sciences, Sofia, Bulgaria). In addition, we thank Hussain Abbas who provided programming support and facilitated the use of the Euler HPC cluster. This study is part of the PhD project by Yannek Käber and was funded by ETH Zurich (Grant ETH-35 18-1).

### **Author contribution**

YK, FH, and HB conceived the idea, developed the concept of this study; YK led the writing of the paper, conducted the analysis, and created the graphics. FH provided statistical support. HB secured funding. All authors contributed to paper writing.

### **Competing interests**

The authors declare that they have no conflict of interest.

### **References**

Andivia, E., Madrigal-González, J., Villar-Salvador, P., and Zavala, M. A.: Do adult trees increase conspecific juvenile resilience to recurrent droughts? Implications for forest regeneration, *Ecosphere*, 9, e02282, <https://doi.org/10.1002/ecs2.2282>, 2018.

Augustynczyk, A. L. D., Hartig, F., Minunno, F., Kahle, H.-P., Diaconu, D., Hanewinkel, M., and Yousefpour, R.: Productivity of *Fagus sylvatica* under climate change – A Bayesian analysis of risk and uncertainty using the model 3-PG, *For. Ecol. Manag.*, 401, 192–206, <https://doi.org/10.1016/J.FORECO.2017.06.061>, 2017.

Botkin, D. B., Janak, J. F., and Wallis, J. R.: Some Ecological Consequences of a Computer Model of Forest Growth, *J. Ecol.*, 60, 849–849, <https://doi.org/10.2307/2258570>, 1972.

- ter Braak, C. J. F. and Vrugt, J. A.: Differential Evolution Markov Chain with snooker updater and fewer chains, *Stat. Comput.*, 18, 435–446, <https://doi.org/10.1007/s11222-008-9104-9>, 2008.
- 695 Bröcker, J. and Smith, L. A.: Scoring Probabilistic Forecasts: The Importance of Being Proper, *Weather Forecast.*, 22, 382–388, <https://doi.org/10.1175/WAF966.1>, 2007.
- Brooks, M. E., Kristensen, K., Benthem, K. J. van, Magnusson, A., Berg, C. W., Nielsen, A., Skaug, H. J., Maechler, M., and Bolker, B. M.: glmmTMB Balances Speed and Flexibility Among Packages for Zero-inflated Generalized Linear Mixed Modeling, *R J.*, 9, 378–400, 2017.
- 700 Bugmann, H.: On the ecology of mountainous forests in a changing climate: a simulation study, PhD Thesis, 1994.
- Bugmann, H. and Cramer, W.: Improving the behaviour of forest gap models along drought gradients, *For. Ecol. Manag.*, 103, 247–263, [https://doi.org/10.1016/S0378-1127\(97\)00217-X](https://doi.org/10.1016/S0378-1127(97)00217-X), 1998.
- Bugmann, H. and Seidl, R.: The evolution, complexity and diversity of models of long-term forest dynamics, *J. Ecol.*, 110, 2288–2307, <https://doi.org/10.1111/1365-2745.13989>, 2022.
- 705 Bugmann, H. and Solomon, A. M.: Explaining Forest Composition and Biomass Across Multiple Biogeographical Regions, *Ecol. Appl.*, 10, 95–114, [https://doi.org/10.1890/1051-0761\(2000\)010\[0095:EFCABA\]2.0.CO;2](https://doi.org/10.1890/1051-0761(2000)010[0095:EFCABA]2.0.CO;2), 2000.
- Chalmandrier, L., Hartig, F., Laughlin, D. C., Lischke, H., Pichler, M., Stouffer, D. B., and Pellissier, L.: Linking functional traits and demography to model species-rich communities, *Nat. Commun.*, 12, 2724, <https://doi.org/10.1038/s41467-021-22630-1>, 2021.
- 710 Clark, J. S., Beckage, B., Camill, P., Cleveland, B., HilleRisLambers, J., Lichter, J., McLachlan, J., Mohan, J., and Wyckoff, P.: Interpreting recruitment limitation in forests, *Am. J. Bot.*, 86, 1–16, <https://doi.org/10.2307/2656950>, 1999.
- Clark, J. S., Iverson, L., Woodall, C. W., Allen, C. D., Bell, D. M., Bragg, D. C., D’Amato, A. W., Davis, F. W., Hersh, M. H., Ibanez, I., Jackson, S. T., Matthews, S., Pederson, N., Peters, M., Schwartz, M. W., Waring, K. M., and Zimmermann, N. E.: The impacts of increasing drought on forest dynamics, structure, and biodiversity in the United States, *Glob. Change Biol.*, 22, 2329–2352, <https://doi.org/10.1111/gcb.13160>, 2016.
- 715 Collins, S. L. and Good, R. E.: The Seedling Regeneration Niche: Habitat Structure of Tree Seedlings in an Oak-Pine Forest, *Oikos*, 48, 89–98, <https://doi.org/10.2307/3565692>, 1987.
- Csilléry, K., Blum, M. G. B., Gaggiotti, O. E., and François, O.: Approximate Bayesian Computation (ABC) in practice, *Trends Ecol. Amp Evol.*, 25, 410–418, <https://doi.org/10.1016/J.TREE.2010.04.001>, 2010.
- 720 Delpierre, N., Lireux, S., Hartig, F., Camarero, J. J., Cheaib, A., Čufar, K., Cuny, H., Deslauriers, A., Fonti, P., Gričar, J., Huang, J.-G., Krause, C., Liu, G., de Luis, M., Mäkinen, H., del Castillo, E. M., Morin, H., Nöjd, P., Oberhuber, W., Prislán, P., Rossi, S., Saderi, S. M., Treml, V., Vavrick, H., and Rathgeber, C. B. K.: Chilling and forcing temperatures interact to predict the onset of wood formation in Northern Hemisphere conifers, *Glob. Change Biol.*, 25, 1089–1105, <https://doi.org/10.1111/gcb.14539>, 2019.

- Detto, M., Levine, J. M., and Pacala, S. W.: Maintenance of high diversity in mechanistic forest dynamics models of competition for light, *Ecol. Monogr.*, 92, e1500, <https://doi.org/10.1002/ecm.1500>, 2022.
- 730 Díaz-Yáñez, O., Käber, Y., Anders, T., Braziunas, K. H., Bruna, J., Fischer, S., Hetzer, J., Hickler, T., Hochauer, C., Lexer, M., Lischke, H., Mahnken, M., Mairota, P., Merganicova, K., Mette, T., Morin, X., Rammer, W., Scheiter, S., Scherrer, D., and Bugmann, H.: Tree regeneration in models of forest dynamics: a key priority for further research, in press.
- Didion, M., Kupferschmid, A. D., Zingg, A., Fahse, L., and Bugmann, H.: Gaining local accuracy while not losing generality — extending the range of gap model applications, *Can. J. For. Res.*, 39, 1092–1107, <https://doi.org/10.1139/X09-041>, 2009a.
- 735 Didion, M., Kupferschmid, A. D., and Bugmann, H.: Long-term effects of ungulate browsing on forest composition and structure, *For. Ecol. Manag.*, <https://doi.org/10.1016/j.foreco.2009.06.006>, 2009b.
- Dietze, M. C.: *Ecological Forecasting*, Princeton University Press, <https://doi.org/10.2307/j.ctvc7796h>, 2017.
- Ellenberg, H.: *Vegetation Mitteleuropas mit den Alpen*, 4th ed., Verlag Eugen Ulmer, Stuttgart, Germany, 1986.
- Ellenberg, H. and Klötzli, F.: *Waldgesellschaften und waldstandorte der schweiz*, Eidgenössische Anstalt f. d.  
740 Forstl. Versuchswesen, 1972.
- Grant, K., Kreyling, J., Heilmeier, H., Beierkuhnlein, C., and Jentsch, A.: Extreme weather events and plant–plant interactions: shifts between competition and facilitation among grassland species in the face of drought and heavy rainfall, *Ecol. Res.*, 29, 991–1001, <https://doi.org/10.1007/s11284-014-1187-5>, 2014.
- Grime, J. P.: Evidence for the Existence of Three Primary Strategies in Plants and Its Relevance to Ecological and  
745 Evolutionary Theory, *Am. Nat.*, 111, 1169–1194, <https://doi.org/10.1086/283244>, 1977.
- Grime, J. P. and Mackey, J. M. L.: The role of plasticity in resource capture by plants, *Evol. Ecol.*, 16, 299–307, <https://doi.org/10.1023/A:1019640813676>, 2002.
- Grossiord, C.: Having the right neighbors: how tree species diversity modulates drought impacts on forests, *New Phytol.*, 228, 42–49, <https://doi.org/10.1111/nph.15667>, 2020.
- 750 Grubb, P. J.: The maintenance of species-richness in plant communities: The importance of the regeneration niche, *Biol. Rev.*, 52, 107–145, <https://doi.org/10.1111/j.1469-185X.1977.tb01347.x>, 1977.
- Haberstroh, S. and Werner, C.: The role of species interactions for forest resilience to drought, *Plant Biol.*, n/a, <https://doi.org/10.1111/plb.13415>, 2022.
- Hanbury-Brown, A. R., Ward, R. E., and Kueppers, L. M.: Forest regeneration within Earth system models: current  
755 process representations and ways forward, *New Phytol.*, 235, 20–40, <https://doi.org/10.1111/nph.18131>, 2022.
- Hart, S. P., Usinowicz, J., and Levine, J. M.: The spatial scales of species coexistence, *Nat. Ecol. Evol.*, 1, 1066–1073, <https://doi.org/10.1038/s41559-017-0230-7>, 2017.

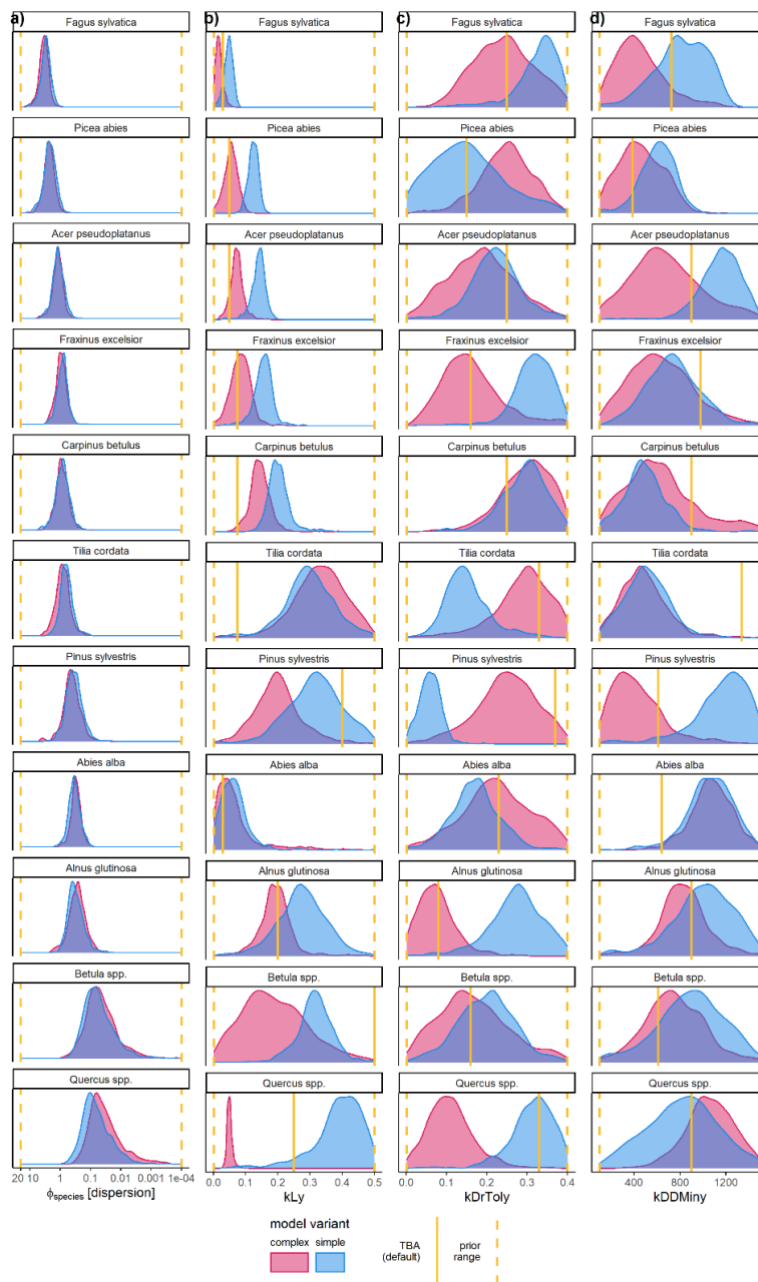
- Hartig, F., Calabrese, J. M., Reineking, B., Wiegand, T., and Huth, A.: Statistical inference for stochastic simulation models - theory and application, *Ecol. Lett.*, 14, 816–827, <https://doi.org/10.1111/j.1461-0248.2011.01640.x>, 2011.
- 760 Hartig, F., Dyke, J., Hickler, T., Higgins, S. I., O’Hara, R. B., Scheiter, S., and Huth, A.: Connecting dynamic vegetation models to data - an inverse perspective, *J. Biogeogr.*, 39, 2240–2252, <https://doi.org/10.1111/j.1365-2699.2012.02745.x>, 2012.
- Hartig, F., Minunno, F., and Paul, S.: *BayesianTools: General-Purpose MCMC and SMC Samplers and Tools for Bayesian Statistics*, 2019.
- 765 Heiland, L., Kunstler, G., Ruiz-Benito, P., Buras, A., Dahlgren, J., and Hülsmann, L.: Divergent occurrences of juvenile and adult trees are explained by both environmental change and ontogenetic effects, *Ecography*, 2022, e06042, <https://doi.org/10.1111/ecog.06042>, 2022.
- Hellegers, M., Ozinga, W. A., Hinsberg van, A., Huijbregts, M. A. J., Hennekens, S. M., Schaminée, J. H. J., Dengler, J., and Schipper, A. M.: Evaluating the ecological realism of plant species distribution models with ecological indicator values, *Ecography*, 43, 161–170, <https://doi.org/10.1111/ecog.04291>, 2020.
- 770 Huber, N., Bugmann, H., and Lafond, V.: Global sensitivity analysis of a dynamic vegetation model: Model sensitivity depends on successional time, climate and competitive interactions, *Ecol. Model.*, 368, 377–390, <https://doi.org/10.1016/J.ECOLMODEL.2017.12.013>, 2018.
- Huber, N., Bugmann, H., and Lafond, V.: Capturing ecological processes in dynamic forest models: why there is  
775 no silver bullet to cope with complexity, *Ecosphere*, 11, <https://doi.org/10.1002/ecs2.3109>, 2020.
- Jucker, T., Bouriaud, O., Avacaritei, D., Dănilă, I., Duduman, G., Valladares, F., and Coomes, D. A.: Competition for light and water play contrasting roles in driving diversity–productivity relationships in Iberian forests, *J. Ecol.*, 102, 1202–1213, <https://doi.org/10.1111/1365-2745.12276>, 2014.
- Käber, Y., Meyer, P., Stillhard, J., Lombaerde, E. D., Zell, J., Stadelmann, G., Bugmann, H., and Bigler, C.: Tree recruitment is determined by stand structure and shade tolerance with uncertain role of climate and water relations,  
780 *Ecol. Evol.*, 11, 12182–12203, <https://doi.org/10.1002/ece3.7984>, 2021.
- Käber, Y., Bigler, C., HilleRisLambers, J., Hobi, M., Nagel, T. A., Aakala, T., Blaschke, M., Brang, P., Brzeziecki, B., Carrer, M., Cateau, E., Frank, G., Fraver, S., Idoate-Lacasia, J., Holik, J., Kucbel, S., Leyman, A., Meyer, P., Motta, R., Samonil, P., Seebach, L., Stillhard, J., Svoboda, M., Szwagrzyk, J., Vandekerkhove, K., Vostarek, O.,  
785 Zlatanov, T., and Bugmann, H.: Sheltered or suppressed? Tree regeneration in unmanaged European forests, *J. Ecol.*, 111, 2281–2295, <https://doi.org/10.1111/1365-2745.14181>, 2023.
- Kass, R. E. and Raftery, A. E.: Bayes Factors, *J. Am. Stat. Assoc.*, 90, 773–795, <https://doi.org/10.1080/01621459.1995.10476572>, 1995.
- Kienast, F.: *FORECE: A forest succession model for southern Central Europe, United States*, 1987.

- 790 Köhler, P. and Huth, A.: The effects of tree species grouping in tropical rainforest modelling: Simulations with the individual-based model Formind, *Ecol. Model.*, 109, 301–321, [https://doi.org/10.1016/S0304-3800\(98\)00066-0](https://doi.org/10.1016/S0304-3800(98)00066-0), 1998.
- König, L. A., Mohren, F., Schelhaas, M.-J., Bugmann, H., and Nabuurs, G.-J.: Tree regeneration in models of forest dynamics – Suitability to assess climate change impacts on European forests, *For. Ecol. Manag.*, 520, 120390, <https://doi.org/10.1016/j.foreco.2022.120390>, 2022.
- 795 Larcher, W.: Physiological plant ecology, *Acta Physiol. Plant.*, 18, 183–184, 1996.
- Lett, S. and Dorrepaal, E.: Global drivers of tree seedling establishment at alpine treelines in a changing climate, *Funct. Ecol.*, 32, 1666–1680, <https://doi.org/10.1111/1365-2435.13137>, 2018.
- Leuschner, C. and Ellenberg, H.: Ecology of Central European Forests: Vegetation Ecology of Central Europe, Volume I, Springer International Publishing, Cham, <https://doi.org/10.1007/978-3-319-43042-3>, 2017.
- 800 Levine, J. I., Levine, J. M., Gibbs, T., and Pacala, S. W.: Competition for water and species coexistence in phenologically structured annual plant communities, *Ecol. Lett.*, 25, 1110–1125, <https://doi.org/10.1111/ele.13990>, 2022.
- Li, Y., Jiang, Y., Zhao, K., Chen, Y., Wei, W., Shipley, B., and Chu, C.: Exploring trait–performance relationships of tree seedlings along experimentally manipulated light and water gradients, *Ecology*, 103, e3703, <https://doi.org/10.1002/ecy.3703>, 2022.
- 805 Lortie, C. J. and Callaway, R. M.: Re-analysis of meta-analysis: support for the stress-gradient hypothesis, *J. Ecol.*, 94, 7–16, <https://doi.org/10.1111/j.1365-2745.2005.01066.x>, 2006.
- Lyr, H., Fiedler, H.-J., and Tranquillini, W.: Physiologie und ökologie der gehölze, Fisch. Jena, 1992.
- 810 Mauri, A., Girardello, M., Strona, G., Beck, P. S. A., Forzieri, G., Caudullo, G., Manca, F., and Cescatti, A.: EU-Trees4F, a dataset on the future distribution of European tree species, *Sci. Data*, 9, 37, <https://doi.org/10.1038/s41597-022-01128-5>, 2022.
- 815 McDowell, N. G., Allen, C. D., Anderson-Teixeira, K., Aukema, B. H., Bond-Lamberty, B., Chini, L., Clark, J. S., Dietze, M., Grossiord, C., Hanbury-Brown, A., Hurtt, G. C., Jackson, R. B., Johnson, D. J., Kueppers, L., Lichstein, J. W., Ogle, K., Poulter, B., Pugh, T. A. M., Seidl, R., Turner, M. G., Uriarte, M., Walker, A. P., and Xu, C.: Pervasive shifts in forest dynamics in a changing world, *Science*, 368, eaaz9463, <https://doi.org/10.1126/science.aaz9463>, 2020.
- Meusel, H., Weinert, E., and Jäger, E.: Vergleichende chorologie der zentraleuropäischen flora, G. Fischer, 1965.
- 820 Morin, X. and Thuiller, W.: Comparing niche- and process-based models to reduce prediction uncertainty in species range shifts under climate change, *Ecology*, 90, 1301–1313, <https://doi.org/10.1890/08-0134.1>, 2009.
- Müller, M. J.: Selected climatic data for a global set of standard stations for vegetation science, Springer Netherlands, Dordrecht, <https://doi.org/10.1007/978-94-009-8040-2>, 1982.

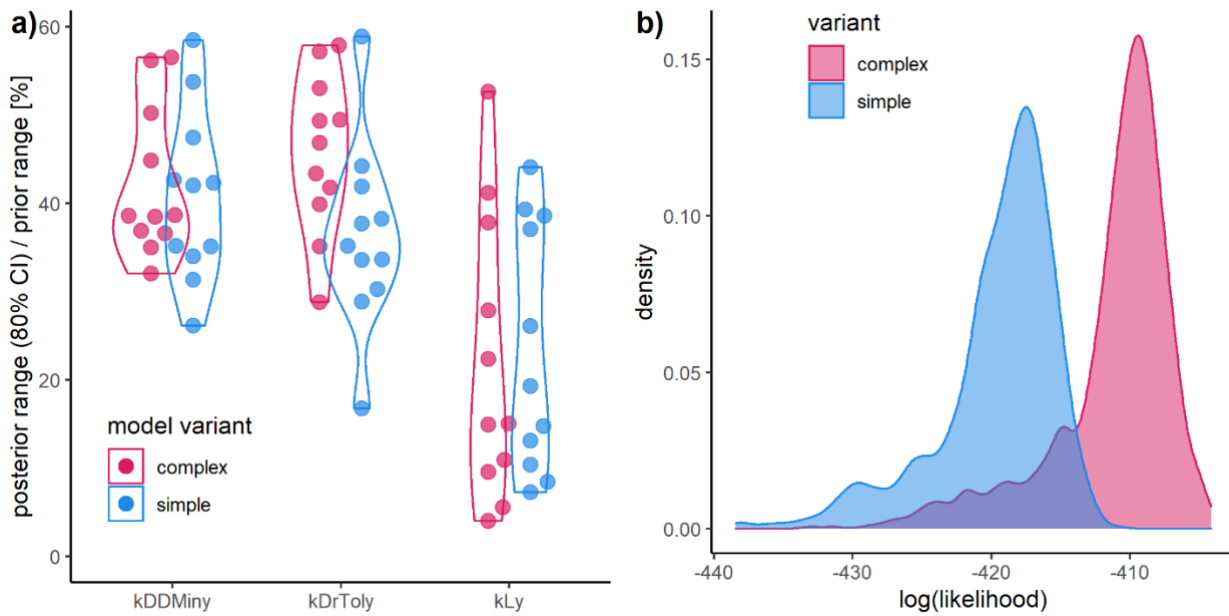
- Oberpriller, J., Cameron, D. R., Dietze, M. C., and Hartig, F.: Towards robust statistical inference for complex computer models, *Ecol. Lett.*, 24, 1251–1261, <https://doi.org/10.1111/ele.13728>, 2021.
- 825 O’Hagan, A.: Fractional Bayes Factors for Model Comparison, *J. R. Stat. Soc. Ser. B Methodol.*, 57, 99–118, <https://doi.org/10.1111/j.2517-6161.1995.tb02017.x>, 1995.
- Paine, C. E. T., Amisshah, L., Auge, H., Baraloto, C., Baruffol, M., Bourland, N., Bruelheide, H., Dainou, K., Gouvenain, R. C. de, Doucet, J.-L., Doust, S., Fine, P. V. A., Fortunel, C., Haase, J., Holl, K. D., Jactel, H., Li, X., Kitajima, K., Koricheva, J., Martínez-Garza, C., Messier, C., Paquette, A., Philipson, C., Piotto, D., Poorter, L., Posada, J. M., Potvin, C., Rainio, K., Russo, S. E., Ruiz-Jaen, M., Scherer-Lorenzen, M., Webb, C. O., Wright, S. J., Zahawi, R. A., and Hector, A.: Globally, functional traits are weak predictors of juvenile tree growth, and we do not know why, *J. Ecol.*, 103, 978–989, <https://doi.org/10.1111/1365-2745.12401>, 2015.
- 830 Price, D. T., Zimmermann, N. E., van der Meer, P. J., Lexer, M. J., Leadley, P., Jorritsma, I. T. M., Schaber, J., Clark, D. F., Lasch, P., McNulty, S., Wu, J., and Smith, B.: Regeneration in Gap Models: Priority Issues for Studying Forest Responses to Climate Change, *Clim. Change*, 51, 475–508, <https://doi.org/10.1023/A:1012579107129>, 2001.
- Risch, A. C., Heiri, C., and Bugmann, H.: Simulating structural forest patterns with a forest gap model: a model evaluation, *Ecol. Model.*, 181, 161–172, <https://doi.org/10.1016/j.ecolmodel.2004.06.029>, 2005.
- Rudloff, W.: *World climates*, Wissenschaftliche Verlagsgesellschaft, 1981.
- 840 Rüger, N., Huth, A., Hubbell, S. P., and Condit, R.: Response of recruitment to light availability across a tropical lowland rain forest community, *J. Ecol.*, 97, 1360–1368, <https://doi.org/10.1111/j.1365-2745.2009.01552.x>, 2009.
- Ruiz-Benito, P., Lines, E. R., Gómez-Aparicio, L., Zavala, M. A., and Coomes, D. A.: Patterns and Drivers of Tree Mortality in Iberian Forests: Climatic Effects Are Modified by Competition, *PLOS ONE*, 8, e56843, <https://doi.org/10.1371/journal.pone.0056843>, 2013.
- 845 Scherrer, D., Vitasse, Y., Guisan, A., Wohlgemuth, T., and Lischke, H.: Competition and demography rather than dispersal limitation slow down upward shifts of trees’ upper elevation limits in the Alps, *J. Ecol.*, 108, 2416–2430, <https://doi.org/10.1111/1365-2745.13451>, 2020.
- Seidl, R. and Turner, M. G.: Post-disturbance reorganization of forest ecosystems in a changing world, *Proc. Natl. Acad. Sci.*, 119, e2202190119, <https://doi.org/10.1073/pnas.2202190119>, 2022.
- 850 Seidl, R., Rammer, W., Scheller, R. M., and Spies, T. A.: An individual-based process model to simulate landscape-scale forest ecosystem dynamics, *Ecol. Model.*, 231, 87–100, <https://doi.org/10.1016/J.ECOLMODEL.2012.02.015>, 2012.
- 855 Shoemaker, L. G., Sullivan, L. L., Donohue, I., Cabral, J. S., Williams, R. J., Mayfield, M. M., Chase, J. M., Chu, C., Harpole, W. S., Huth, A., HilleRisLambers, J., James, A. R. M., Kraft, N. J. B., May, F., Muthukrishnan, R., Satterlee, S., Taubert, F., Wang, X., Wiegand, T., Yang, Q., and Abbott, K. C.: Integrating the underlying structure of stochasticity into community ecology, *Ecology*, 101, e02922, <https://doi.org/10.1002/ecy.2922>, 2020.

- Shugart, H. H.: *A Theory of Forest Dynamics: The Ecological Implications of Forest Succession Models*, 1984.
- Smith, P., Beven, K. J., and Tawn, J. A.: Informal likelihood measures in model assessment: Theoretic development and investigation, *Adv. Water Resour.*, 31, 1087–1100, <https://doi.org/10.1016/j.advwatres.2008.04.012>, 2008.
- 860 Svenning, J.-C., Normand, S., and Skov, F.: Postglacial dispersal limitation of widespread forest plant species in nemoral Europe, *Ecography*, 31, 316–326, <https://doi.org/10.1111/j.0906-7590.2008.05206.x>, 2008.
- Thakur, M. P. and Wright, A. J.: Environmental Filtering, Niche Construction, and Trait Variability: The Missing Discussion, *Trends Ecol. Evol.*, 32, 884–886, <https://doi.org/10.1016/j.tree.2017.09.014>, 2017.
- 865 Trotsiuk, V., Hartig, F., Cailleret, M., Babst, F., Forrester, D. I., Baltensweiler, A., Buchmann, N., Bugmann, H., Gessler, A., Gharun, M., Minunno, F., Rigling, A., Rohner, B., Stillhard, J., Thuerig, E., Waldner, P., Ferretti, M., Eugster, W., and Schaub, M.: Assessing the response of forest productivity to climate extremes in Switzerland using model-data fusion, *Glob. Change Biol.*, gcb.15011-gcb.15011, <https://doi.org/10.1111/gcb.15011>, 2020.
- Van Oijen, M., Rougier, J., and Smith, R.: Bayesian calibration of process-based forest models: bridging the gap between models and data, *Tree Physiol.*, 25, 915–927, <https://doi.org/10.1093/treephys/25.7.915>, 2005.
- 870 Vincent, G. and Harja, D.: Exploring Ecological Significance of Tree Crown Plasticity through Three-dimensional Modelling, *Ann. Bot.*, 101, 1221–1231, <https://doi.org/10.1093/aob/mcm189>, 2008.
- Vitasse, Y.: Ontogenic changes rather than difference in temperature cause understory trees to leaf out earlier, *New Phytol.*, 198, 149–155, <https://doi.org/10.1111/nph.12130>, 2013.
- 875 Welden, C. W. and Slauson, W. L.: The Intensity of Competition Versus its Importance: An Overlooked Distinction and Some Implications, *Q. Rev. Biol.*, 61, 23–44, <https://doi.org/10.1086/414724>, 1986.
- Werner, E. E. and Gilliam, J. F.: The Ontogenetic Niche and Species Interactions in Size-Structured Populations, *Annu. Rev. Ecol. Syst.*, 15, 393–425, <https://doi.org/10.1146/annurev.es.15.110184.002141>, 1984.
- Wood, S. N.: Statistical inference for noisy nonlinear ecological dynamic systems, *Nature*, 466, 1102–1104, <https://doi.org/10.1038/nature09319>, 2010.
- 880 Yang, J., Cao, M., and Swenson, N. G.: Why Functional Traits Do Not Predict Tree Demographic Rates, *Trends Ecol. Evol.*, 33, 326–336, <https://doi.org/10.1016/j.tree.2018.03.003>, 2018.
- Young, D. J. N., Stevens, J. T., Earles, J. M., Moore, J., Ellis, A., Jirka, A. L., and Latimer, A. M.: Long-term climate and competition explain forest mortality patterns under extreme drought, *Ecol. Lett.*, 20, 78–86, <https://doi.org/10.1111/ele.12711>, 2017.
- 885 Zell, J., Rohner, B., Thürig, E., and Stadelmann, G.: Modeling ingrowth for empirical forest prediction systems, *For. Ecol. Manag.*, 433, 771–779, <https://doi.org/10.1016/j.foreco.2018.11.052>, 2019.

# Appendix A

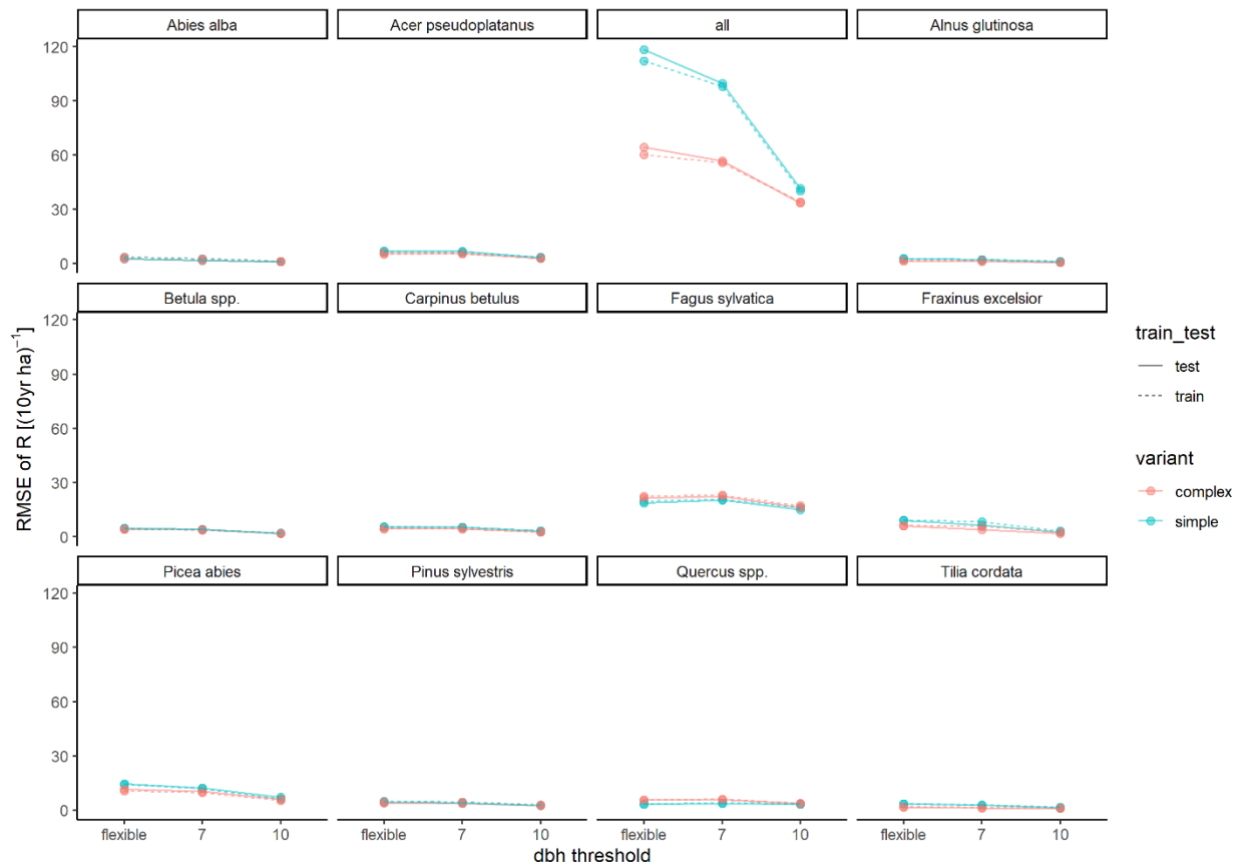


890 **Figure A1: Posterior distribution of species-specific parameters for the complex model (red) and the simple model (blue). The first column a) shows the species-specific dispersion parameter  $\phi$ . The other columns show the ecological regeneration thresholds: b) light requirements (kLy), c) drought tolerance (kDrToly), and d) degree-days (kDDMiny). The species are sorted row-wise according to their average dispersion across both models. The prior parameter range and the expected value are indicated by the dashed and solid yellow lines, respectively.**

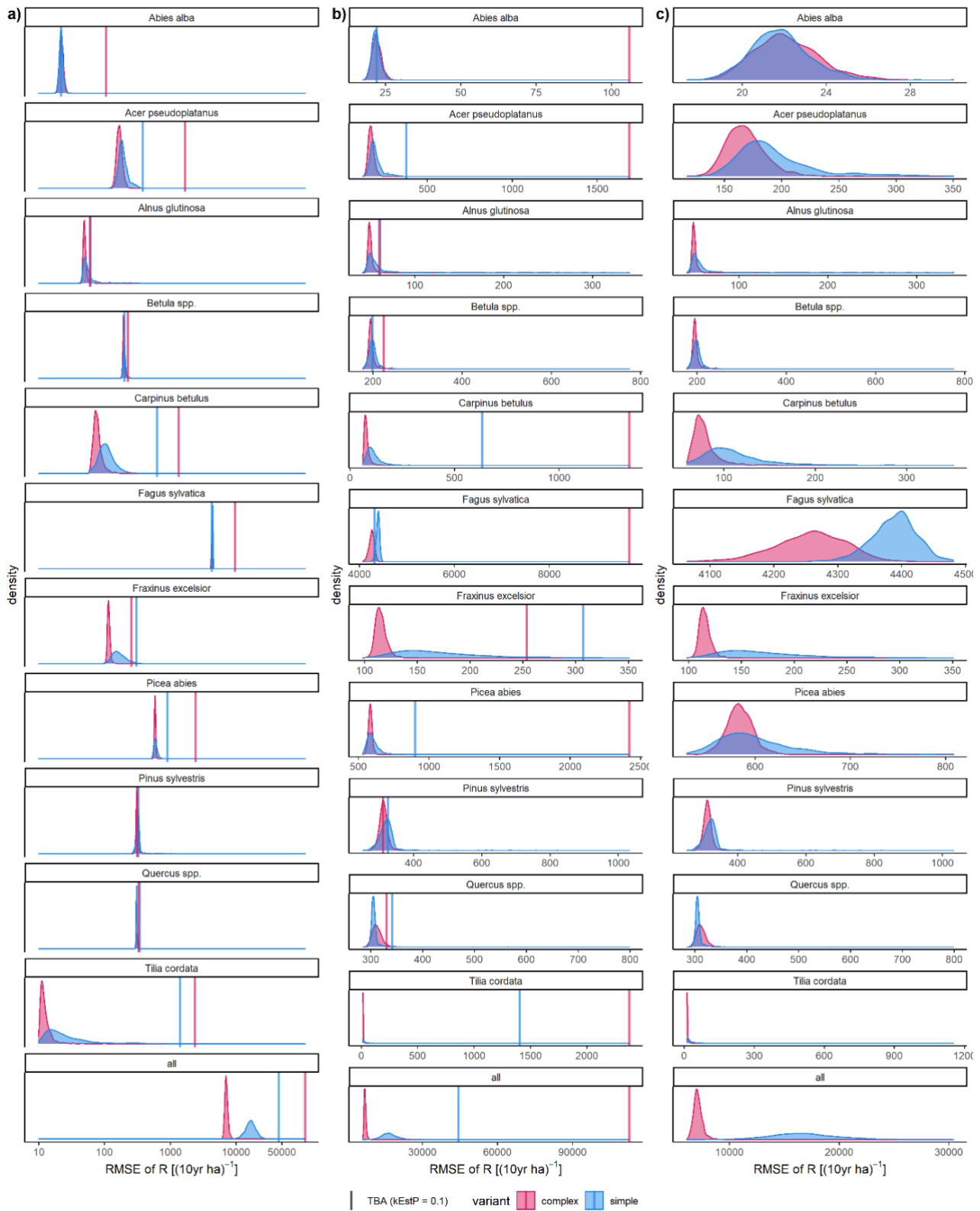


895

**Figure A2:** a) Sensitivity of the parameters expressed by the percentage of the prior range that is covered by the 80% CI. b) Likelihood distribution of the posterior simulations from the simple model (blue) and the complex model (red). The results for the complex and the simple model are shown in red and blue, respectively.



900 **Figure A3: Relationship between RMSE and DBH threshold.** “flexible” refers to the individual DBH thresholds applied during model calibration. 7 and 10 cm comprise the subset of sites which had at least 7 or 10 cm DBH, respectively.



905

**Figure A4: Root mean squared error (RMSE) of the difference between posterior predictions ( $\hat{R}$ ) and observations (R). Axis scaling differs between a) log10 scaled, b) varying x axis range with the trait-based approach TBA (default) RMSE, c) varying x axis only inverse calibration (ICA) posterior.**

**Table A1: Posterior values of the recruitment amount parameters kTrMax (complex model) and kEstDens (simple model), and the effects of DBH  $\phi_{DBH}$  and plot area  $\phi_A$  on dispersion. Where the outer values refer to the 80 % CIs and the middle values refers to the MPE. 10%CI | MPE | 90%CI**

	$\phi_{DBH}$	$\phi_A$	kTrMax		kEstDens	
			ICA	TBA	ICA	TBA
complex	-0.439 -0.388 -0.346	-0.345 -0.171 -0.002	7372 8762 10210	50000	-	-
simple	-0.473 -0.405 -0.345	-0.261 -0.120 0.017	-	-	0.017 0.022 0.027	0.006

910

**Table A2: Species posterior parameter values for light requirements (kL<sub>y</sub>), drought tolerance (kDrTol<sub>y</sub>), and degree-days (kDDMin<sub>y</sub>) including its default values. Where the outer values refer to the 80 % CIs and the middle values refers to the MPE. 10%CI | MPE | 90%CI. \* Default values for Betula spp. are those of Betula pendula, default values for Quercus spp. are those of Quercus petraea.**

species	kL <sub>y</sub>			kDrTol <sub>y</sub>			kDDMin <sub>y</sub>		
	TBA	ICA		TBA	ICA		TBA	ICA	
		10%CI   MPE   90%CI			10%CI   MPE   90%CI			10%CI   MPE   90%CI	
		simple	complex		simple	complex		simple	complex
<i>Abies alba</i>	0.03	0.02 0.07 0.12	0.01 0.07 0.15	0.23	0.10 0.17 0.25	0.11 0.22 0.34	641	810 1058 1301	844 1072 1292
<i>Acer pseudoplatanus</i>	0.05	0.11 0.14 0.16	0.05 0.07 0.10	0.25	0.15 0.22 0.30	0.08 0.18 0.29	898	927 1148 1365	305 677 1091
<i>Alnus glutinosa</i>	0.2	0.18 0.27 0.37	0.13 0.19 0.25	0.08	0.19 0.27 0.35	0.02 0.08 0.14	898	661 997 1325	576 827 1092
<i>Betula</i> spp.*	0.5	0.25 0.32 0.38	0.07 0.19 0.33	0.16	0.11 0.20 0.29	0.06 0.17 0.28	610	512 892 1265	427 752 1054
<i>Carpinus betulus</i>	0.075	0.17 0.20 0.24	0.11 0.14 0.18	0.25	0.22 0.29 0.36	0.21 0.30 0.37	898	260 496 736	260 626 1051
<i>Fagus sylvatica</i>	0.03	0.03 0.05 0.06	0.01 0.02 0.03	0.25	0.26 0.32 0.38	0.14 0.24 0.34	723	506 811 1094	204 454 745
<i>Fraxinus excelsior</i>	0.075	0.12 0.15 0.19	0.05 0.08 0.12	0.16	0.26 0.31 0.37	0.08 0.16 0.26	980	443 737 1040	293 635 996
<i>Picea abies</i>	0.05	0.10 0.12 0.14	0.03 0.05 0.08	0.15	0.04 0.15 0.28	0.16 0.25 0.33	385	416 603 782	208 461 720
<i>Pinus sylvestris</i>	0.4	0.20 0.31 0.42	0.11 0.20 0.30	0.37	0.02 0.06 0.09	0.15 0.25 0.34	610	828 1147 1419	180 432 719
<i>Quercus</i> spp.*	0.2	0.28 0.39 0.47	0.04 0.05 0.06	0.33	0.24 0.31 0.38	0.05 0.11 0.19	785	394 820 1213	787 1056 1328
<i>Tilia cordata</i>	0.075	0.20 0.30 0.39	0.23 0.33 0.43	0.33	0.09 0.15 0.22	0.20 0.29 0.37	1339	260 512 752	246 487 735

915 **Table A3: Species dispersion parameter posterior values. Where the outer values refer to the 80 % CIs and the middle values refers to the MPE. 10%CI | MPE | 90%CI**

species	complex	simple
<i>Abies alba</i>	0.010 0.018 0.025	0.011 0.019 0.028
<i>Acer pseudoplatanus</i>	0.043 0.072 0.102	0.038 0.064 0.092
<i>Alnus glutinosa</i>	0.008 0.018 0.031	0.008 0.018 0.030
<i>Betula</i> spp.	0.001 0.004 0.008	0.001 0.004 0.009
<i>Carpinus betulus</i>	0.028 0.052 0.077	0.028 0.048 0.069
<i>Fagus sylvatica</i>	0.141 0.199 0.257	0.117 0.161 0.208
<i>Fraxinus excelsior</i>	0.035 0.055 0.080	0.029 0.047 0.064
<i>Picea abies</i>	0.087 0.135 0.182	0.081 0.121 0.165
<i>Pinus sylvestris</i>	0.013 0.026 0.040	0.009 0.021 0.032
<i>Quercus</i> spp.	0.000 0.003 0.006	0.001 0.005 0.010
<i>Tilia cordata</i>	0.026 0.051 0.080	0.019 0.036 0.054

**Table A4: Gelman-rubin diagnostics for the simple and complex model split by the two sets of independent chains. For visual inspection of the chains see the traceplots in the dedicated file.**

	simple model				complex model			
	chains 1-3		chains 4-6		chains 1-3		chains 4-6	
	Point est.	Upper C.I.	Point est.	Upper C.I.	Point est.	Upper C.I.	Point est.	Upper C.I.
kEstDens/kTrMax	1.001	1.002	1.034	1.050	1.004	1.015	1.073	1.090
dispdbh	1.000	1.000	1.232	1.657	1.002	1.003	1.274	1.761
disppsize	1.000	1.000	1.058	1.146	1.002	1.009	1.238	1.672
kDDMiny_0	1.001	1.003	1.053	1.153	1.004	1.011	1.044	1.050
kDDMiny_2	1.002	1.006	1.115	1.239	1.000	1.001	1.022	1.056
kDDMiny_5	1.005	1.011	1.251	1.780	1.000	1.000	1.212	1.597
kDDMiny_9	1.003	1.008	1.124	1.255	1.001	1.005	1.245	1.719
kDDMiny_10	1.001	1.005	1.096	1.175	1.002	1.006	1.057	1.091
kDDMiny_13	1.002	1.006	1.074	1.098	1.002	1.006	1.034	1.055
kDDMiny_14	1.007	1.022	1.204	1.618	1.002	1.008	1.067	1.168
kDDMiny_17	1.002	1.005	1.065	1.171	1.003	1.013	1.156	1.444
kDDMiny_18	1.001	1.003	1.108	1.274	1.004	1.014	1.164	1.474
kDDMiny_21	1.001	1.001	1.034	1.035	1.005	1.017	1.031	1.053
kDDMiny_27	1.002	1.005	1.314	1.995	1.001	1.002	1.211	1.640
kDrToly_0	1.004	1.010	1.080	1.088	1.003	1.007	1.025	1.030
kDrToly_2	1.000	1.000	1.092	1.244	1.012	1.038	1.027	1.040
kDrToly_5	1.004	1.011	1.138	1.325	1.000	1.001	1.101	1.228
kDrToly_9	1.002	1.006	1.082	1.218	1.002	1.006	1.057	1.114
kDrToly_10	1.001	1.004	1.108	1.273	1.003	1.009	1.324	2.116
kDrToly_13	1.001	1.003	1.058	1.091	1.001	1.004	1.041	1.052
kDrToly_14	1.001	1.002	1.222	1.681	1.000	1.001	1.071	1.167
kDrToly_17	1.005	1.011	1.156	1.435	1.001	1.002	1.039	1.057
kDrToly_18	1.004	1.007	1.284	1.981	1.002	1.008	1.176	1.504
kDrToly_21	1.000	1.001	1.003	1.005	1.001	1.006	1.083	1.195
kDrToly_27	1.001	1.006	1.182	1.530	1.002	1.006	1.228	1.676
kLy_0	1.003	1.007	1.252	1.876	1.005	1.009	1.403	2.317
kLy_2	1.002	1.005	1.138	1.280	1.002	1.003	1.030	1.039
kLy_5	1.003	1.007	1.090	1.194	1.002	1.007	1.142	1.389
kLy_9	1.007	1.014	1.190	1.559	1.000	1.001	1.037	1.060
kLy_10	1.004	1.010	1.072	1.074	1.009	1.032	1.232	1.754
kLy_13	1.002	1.004	1.110	1.235	1.004	1.012	1.112	1.289
kLy_14	1.001	1.005	1.243	1.819	1.000	1.001	1.077	1.091
kLy_17	1.000	1.001	1.034	1.093	1.001	1.002	1.037	1.062
kLy_18	1.002	1.003	1.145	1.164	1.001	1.003	1.042	1.053
kLy_21	1.006	1.013	1.210	1.643	1.001	1.004	1.066	1.115
kLy_27	1.001	1.002	1.137	1.345	1.001	1.002	1.059	1.098
disp_0	1.000	1.001	1.238	1.747	1.001	1.001	1.234	1.726
disp_2	1.000	1.000	1.237	1.727	1.002	1.004	1.343	2.168
disp_5	1.001	1.002	1.214	1.635	1.006	1.011	1.296	2.079
disp_9	1.001	1.001	1.222	1.700	1.001	1.002	1.239	1.725
disp_10	1.000	1.001	1.267	1.992	1.003	1.008	1.287	1.934
disp_13	1.004	1.009	1.228	1.730	1.030	1.060	1.230	1.727
disp_14	1.000	1.000	1.290	1.966	1.002	1.005	1.236	1.723
disp_17	1.000	1.000	1.246	1.740	1.007	1.015	1.358	2.096
disp_18	1.002	1.003	1.140	1.389	1.006	1.020	1.343	2.229
disp_21	1.012	1.022	1.276	2.006	1.004	1.008	1.174	1.501
disp_27	1.003	1.008	1.237	1.761	1.001	1.002	1.309	2.242

disp\_999

1.002

1.002

1.342

2.195

1.002

1.005

1.397

2.197

## Appendix B Model description

925 This Appendix provides a detailed description of the two model variants used in this study. It complements the description in the main script (Figure 1) but only covers the regeneration module of ForClim. Note that this model incorporates some minor changes compared to the original formulations in Bugmann (1994) for the simple model and Huber et al. (2020) for the complex model. However, these changes do not affect the functioning of the model.

**Table B1: Description of ForClim all model variables and parameters used in this study. Calibrated parameters are explained in more detail in Table 1 in the main text.**

group	variable	unit	description	model	reference
establishment flags	ALEF	boolean	Light availability establishment flag	simple	Bugmann, 1994
	ALEFc	%/100	continuous light availability establishment flag	complex	Bugmann, 1994
	BPEF	boolean	Browsing pressure establishment flag	simple	Bugmann, 1994
	BPEFc	%/100	continuous browsing pressure establishment flag	complex	Bugmann, 1994
	DDEF	boolean	Degree-days establishment flag	simple	Bugmann, 1994
	DDEFc	%/100	continuous degree-days establishment flag	complex	Bugmann, 1994
	SMEF	boolean	Soil moisture establishment flag	simple	Didion et al., 2009a
	SMEFc	%/100	continuous soil moisture establishment flag	complex	Didion et al., 2009a
	WTEF	boolean	Winter temperature establishment flag	simple	Bugmann, 1994
WTEFc	%/100	continuous winter temperature establishment flag	complex	Bugmann, 1994	
general parameter	kDDL	°C·d	annual DD below which DDsum prevents establishment	complex	Bugmann, 1994
	kDDL	°C·d	annual DD above which DDsum is not reducing kTrMax	complex	Bugmann, 1994
	kDrLL	%/100	mDrAn below which drought is not reducing kTrMax	complex	Bugmann, 1994
	kDrUL	%/100	mDrAn above which drought prevents establishment	complex	Bugmann, 1994
	kEstDens	m <sup>-2</sup> ·yr <sup>-1</sup>	Maximum number of tree establishment density	both	Bugmann, 1994
	kEstP	%/100	general probability of regeneration	both	Bugmann, 1994
	kPatchSize	m <sup>2</sup>	size of a forest patch	both	Bugmann, 1994
	kTrMax	ha <sup>-1</sup>	Maximum number of trees per ha	both	Huber et al., 2020
	kDDMin	°C·d	minimum degree-day sum for adults	both	Bugmann, 1994
	kDDMiny	°C·d	minimum degree-day sum for regeneration	both	-
	kDrTol	%/100	drought tolerance for adults	both	Bugmann, 1994
	kDrToly	%/100	drought tolerance for regeneration	both	-
	kL <sub>a</sub>	[1-9]	adult light requirements as proxy for seed production	simple	Risch et al., 2005
kL <sub>y</sub>	%/100	light requirements of regeneration	both	Bugmann, 1994	
state variable (regeneration)	Efc	%/100	minimum continuous establishment flag	complex	Huber et al., 2020
	EFSum	-	sum over all continuous establishment flags	complex	-
	gEstMax	-	annual potential maximum number of established trees	both	Bugmann, 1994
	kEstMax	-	maximum regeneration for a species	simple	Bugmann, 1994
	nTrs	-	the number of trees that are being recruited	both	Bugmann, 1994
	PEst	%/100	realized regeneration probability	both	-
	uEFMax	%/100	helper variable to ensure that Efc is not smaller than 0	complex	-
	ukEstP	%/100	helper variable to calculate PEst in the complex model	complex	-
state variable (site)	gDD	°C·d	mean annual degree days from weather generator	both	Bugmann, 1994
	gDr	%/100	mean annual drought index from weather generator	both	Bugmann, 1994
	gRedFac	%/100	overall reduction factor	complex	Huber et al., 2020
	gRedFacDD	%/100	reduction of kTrMax caused by degree days	complex	Bugmann, 1994
	gRedFacDI	%/100	reduction of kTrMax caused by drought index	complex	Bugmann 1996
	mDDAn	°C·d	mean annual degree days from weather generator	complex	Bugmann 1996

	mDrAn	%/100	mean annual drought index from weather generator	complex	Bugmann 1996
state variable	gAL0	%/100	available light at the forest floor	both	Bugmann 1996
(stand)	Trs	-	N of trees of all species in current simulation year	both	Bugmann 1996

930 **Step 1 – Does regeneration take place?**

First, it is determined whether regeneration takes place at all in any given year; this is done for each species on each patch. The probability of regeneration (kEstP) was set to 2% for the calibration, lower than the default value of kEstP of the default model (trait-based approach) (10%). This was done to reduce the number of cohorts and thus computational costs. The reduction, however, does not reduce effective regeneration because it can be compensated by the parameters for the regeneration amount (kEstDens and kTrMax; cf. Table B1 and eq. A3 and eq. A4), in the sense that a reduction of kEstP by a factor of 1/5, for example, can be compensated by an increase of kEstDens or kTrMax by a factor of 5.

$$PEst_s = kEstP \times WTEF_s \times ALEF_s \times BPEF_s \times DDEF_s \times SMEF_s$$

$$PEst_s = \begin{cases} 1, & U(0,1) < PEst_s, \\ 0, & \text{else} \end{cases}, \quad \text{eq. A1)}$$

where U is a function that draws a random number from a uniform distribution ranging from 0 to 1. The complex model determines whether regeneration takes place (PEst = 1) or not (PEst = 0) regardless of the species but depending on the site factors degree-days (mDDAn), and drought (mDrAn). Specifically, PEst is calculated with

$$kDrLL = 0.1; kDrUL = 0.5$$

$$kDDUL = 1225; kDDL = 0$$

$$gRedFacDI = \frac{mDrAn - kDrLL}{kDrUL - kDrLL}$$

$$gRedFacDD = 1.0 - \frac{mDDAn - kDDL}{kDDUL - kDDL} \quad \text{eq. A2)}$$

$$gRedFac = \text{Max}(gRedFacDI, gRedFacDD)$$

$$ukEstP = kEstP \times (1 - gRedFac)$$

$$PEst = \begin{cases} 1, & U(0,1) < ukEstP \\ 0, & \text{else} \end{cases}.$$

940

**Step 2 – How much regeneration?**

Second, the number of new trees is calculated.

The **simple model** simulates the maximum regeneration amount per species based on the establishment intensity parameter (kEstDens), but also based on kLa<sub>s</sub> which is used as a proxy for seed production (Huber et al., 2020; Risch et al., 2005). Specifically, the maximum regeneration kEstMax<sub>s</sub> for species s is calculated with

$$kEstMax_s = PEst_s \times kEstDens \times kPatchSize * kLa_{a,s}, \quad \text{eq. A3)}$$

where kPatchSize is patch size, which was set to 800 m<sup>2</sup>.

In the **complex model**, regeneration amount is regulated by the continuous establishment flag (EFc) of the most suitable species, site factors (see calculation of gRedFac in eq. A2), and the regeneration intensity parameter kTrMax, Specifically the regeneration amount over all species (nTrs) is calculated with

$$\begin{aligned}
 \text{EFc}_s &= \text{MIN}(\text{WTEFc}_s, \text{ALEFc}_s, \text{BPEFc}_s, \text{DDEFc}_s, \text{SMEFc}_s) \\
 \text{uEFMax} &= \text{MAX}(0, \text{EFc}_s) \\
 \text{gEstMax} &= \text{PEst} * \text{uEFMax} \times \left( \frac{\text{kTrMax} \times (1 - \text{gRedFac})}{10000 \times \text{kPatchSize}} - \text{Trs} \right) \\
 \text{nTrs} &= \text{U}(1, \text{gEstMax})
 \end{aligned} \tag{eq. A4}$$

### 950 Step 3 – What species?

Third, the final number of new trees for each species (nTrs<sub>s</sub>) is determined.

In the **simple model**, for each species *s* a random number between 1 and kEstMax<sub>s</sub> is drawn with

$$\text{nTrs}_s = \text{U}(1, \text{kEstMax}_s). \tag{eq. A5}$$

In the **complex model**, nTrs<sub>s</sub> is calculated for each species *s* based on its suitability for regeneration (EFc<sub>s</sub>) and relative to the suitability of all other species (EFSum) with

$$\begin{aligned}
 \text{EFSum} &= \sum_{s=1}^n \text{EFc}_s \\
 \text{nTrs}_s &= \frac{\text{nTrs} \times \text{EFc}_s}{\text{EFSum}}
 \end{aligned} \tag{eq. A6}$$

955 Ultimately, nTrs<sub>s</sub> denotes the number of trees with a DBH of 1.27 cm in a new cohort per species *s* on one patch and serves as a basis for calculating the likelihood (see below). After a new cohort has established, it follows the rules of adult growth and mortality, which remain unchanged throughout this study by keeping all model parameters that directly affect trees above a DBH of 1.27 cm at their default (Bugmann, 1994; Huber et al., 2020).

### 960 References

Bugmann, H.: On the ecology of mountainous forests in a changing climate: a simulation study, PhD Thesis, 1994.

Didion, M., Kupferschmid, A. D., Zingg, A., Fahse, L., and Bugmann, H.: Gaining local accuracy while not losing generality — extending the range of gap model applications, *Can. J. For. Res.*, 39, 1092–1107, <https://doi.org/10.1139/X09-041>, 2009.

- 965 Huber, N., Bugmann, H., and Lafond, V.: Capturing ecological processes in dynamic forest models: why there is no silver bullet to cope with complexity, *Ecosphere*, 11, <https://doi.org/10.1002/ecs2.3109>, 2020.
- Risch, A. C., Heiri, C., and Bugmann, H.: Simulating structural forest patterns with a forest gap model: a model evaluation, *Ecol. Model.*, 181, 161–172, <https://doi.org/10.1016/j.ecolmodel.2004.06.029>, 2005.

970